universität wien

MASTERARBEIT

Titel der Masterarbeit

„Proof of concept studies for tumor mimotope vaccines“

Verfasserin

Kathrin Thell

angestrebter akademischer Grad

Master of Science (MSc)

Wien, 2012

Studienkennzahl lt. Studienblatt:	A 066 834
Studienrichtung lt. Studienblatt:	Masterstudium Molekulare Biologie
Betreuerin / Betreuer:	Univ. Prof. Dr. Manuela Baccarini

Danksagung

Als erstes möchte ich mich sehr herzlich bei Frau Univ. Prof. Dr. Erika Jensen-Jarolim bedanken. Du hast mir die Möglichkeit gegeben wissenschaftlich zu arbeiten und mir gezeigt, wie man mit viel Fleiß und Engagement seine Forschungsziele erreichen kann. Weiteres hast du es arrangiert, dass ich an Seminaren, Symposien und Kongressen teilnehmen und selbst dort Forschungsergebnisse präsentieren konnte. Vielen Dank Erika!
Ebenso möchte ich mich hier bei Frau Univ. Prof. Dr. Manuela Baccarini für die kompetente Betreuung erkenntlich zeigen.

Ganz besonderem Dank gelten vor allem Dr. Mag. Krisztina Szalai, Dr. Josef Singer und Anna Willensdorfer. Ihr seid mir jederzeit mit bewundernswertem Wissen und tatkräftiger Unterstützung zur Seite gestanden. Ohne euch wäre diese Arbeit nicht so gut gelungen.

Weiteres möchte ich mich beim gesamten IPA Team bedanken. Ihr habt mich vom ersten Tag an aufgenommen und wart für alle Fragen offen. Danke an:
Univ. Prof. DDr. Isabella Pali-Schöll, Dr. Franziska Roth-Walter, Mag. Caroline Stremnitzer, Dr. Philipp Starkl, Dr. Marlene Weichselbaumer, Mag. Mira Matz, Dr. Beatrix Pfanzagl, Helen Szöllösi, Mag. Anna Lukschal, Mag. Durga Krishnamurthy, Cornelia Schulz, DDr. Susanne Diesner, Univ. Doz. Dr. Eva Untersmayer-Elsenhuber, Vera Lisa Assmann, Kristina Kreiner, Erika Bajna, Teresa Manhart, Univ. Prof. Dr. Diana Mechtcheriakova und allen anderen.

Vielen Dank, Martin. Du hast mich allemal angespornt und mich in auch noch so schwierigen Zeiten aufgeheitert.

Danke Birgit, du hast mir gezeigt, dass man mit Frohsinn und Begeisterung vieles erreichen kann.

Besondere Dankbarkeit gilt jedoch meinen Eltern. Ihr habt mich endlos unterstützt, ermutigt und mir es ermöglicht meine Träume und Ziele zu verwirklichen. Danke für eure Ratschläge, Hilfe und große Geduld!

DANKE EUCH ALLEN!

Index

Zusammenfassung

Brustkrebs, genannt Mammakarzinom, ist eine maligne Veränderung des epithelialen Brustgewebes und repräsentiert eine der bösartigsten und häufigsten Form von Krebs bei Frauen.

Ein signifikanter Teil aller Mammakarzinome weisen eine Überexpression des Humanen Epidermalen Wachstums Faktor Rezeptor-Moleküls HER-2 auf, welches mit aggressivem Krankheitsverlauf und einer ungünstigen Prognose assoziiert ist. HER-2 ist auf der Oberfläche von 30% der Krebszellen bei invasivem Brustkrebs, 70% bei duktalem Carzinoma in situ, aber auch bei Ovarial-, Nieren- und Dickdarmkarzinom überexprimiert. HER-2 Expression ermöglicht eine zielgerichtete Behandlung („targeted therapy“) mit dem humanisierten monoklonalen Antikörper Trastuzumab (Herceptin®) der gegen den extrazellulären Teil des Moleküls gerichtet ist. Probleme, wie ungleichmäßige Verteilung im Gewebe und limitierte Halbwertzeit von IgG Antikörpern und nicht zuletzt hohe Kosten vermindern jedoch die Attraktivität der sonst erfolgreichen passiven Immuntherapie. Daher wäre eine ebenso Epitop-spezifische, aber aktive Immuntherapie eine interessantere Alternative. Nach dem Prinzip von Impfungen gegen Infektionserkrankungen wird weltweit auch an „Impfung gegen Krebs“ gearbeitet. Die durch eine Impfung verstärkte Immunantwort gegen die körpereigenen Tumorantigene wäre besonders hilfreich, um einen Schutz vor Wiederkehren des Tumors oder Metastasierung, beispielsweise im Stadium der minimalen Resterkrankung („minimal residual disease“) zu verhindern.

Mittels Phage-Display Technologie können Mimotope gegen wichtige Tumorantigene generiert werden. Mimotope sind kleine Peptide mit ähnlichen Eigenschaften wie die natürlichen Epitope auf einem Antigen. Mimotope können synthetisch hergestellt und an Carrier-Moleküle gekoppelt werden. Ziel dieser Studie war es, AAVLP (Adeno-Associated Virus-Like Particle) als völlig neuartige Mimotopcarrier auf ihre antigene und immunogene Eigenschaften zu testen und weiters sollte der mögliche inhibierende Effekt eines solchen AAVLP-Mimotope-Vakzines auf das Tumorwachstum getestet werden. AAV (Adeno-assoziierter Virus) ist ein nicht humanpathogener, replikationsdefekter ssDNA Virus, der aus 60 Kopien dreier ähnlicher Kapsidproteine besteht. Wenn Fusionsmoleküle aus Mimotop und einen AAV Kapsidprotein exprimiert werden, können diese zu Virus-like particle, AAVLPs assembliert werden. Fertige AAVLPs präsentieren das Mimotop 60-mal auf der Partikeloberfläche.

In dieser Studie wurden zuerst Immunogenität, Spezifität und die Sicherheitsaspekte einer AAVLP Impfung anhand des Modellallergens Ovalbumin evaluiert. Im zweiten Schritt wurde der anti – Tumoreffekt einer spezifischen HER-2 Mimotop Vakzine, vorerst in AAV Formal, in einem Tumortransplantmodell in BALB/c Mäusen getestet.

Abstract

Breast cancer, alternately termed mamma carcinoma, is a malignant neoplasm deriving from mammary epithelial tissue, and represents one of the most malignant and common forms of cancer in females.

In a significant number of all mammary carcinomas the Human Epidermal growth factor Receptor molecule HER-2 is overexpressed, being associated with aggressive disease course and bad prognosis. HER-2 is expressed on the surface of 30% of invasive breast cancer, in 70% of ductal carcinoma in situ, but also in carcinomas of the ovary, the kidney and the colon. Expression enables targeted therapy with the humanized monoclonal antibody trastuzumab (Herceptin®) that is directed against the extracellular part of HER-2. Problems like inhomogeneous distribution in tissue, limited half-life and last but not least high costs decrease attractiveness of elsewise successful passive immunotherapy with IgG antibodies. For these reasons, equally epitope-specific, but active immunotherapy would be an attractive alternative. According to the principle of vaccination against infectious diseases, worldwide efforts are undertaken to develop anti-cancer vaccines. By vaccines immune responses against (self-) tumor-antigens could be achieved to protect against tumors or metastasis recurring during minimal residual diseases.

Using phage-display technology, mimotopes against important tumor antigens can be generated. Mimotopes are small peptides harboring similar biological and physicochemical properties like the natural epitopes. Mimotopes can be produced synthetically and coupled to carrier molecules. The aim of this study was to test the antigenic and immunogenic properties of AAVLPs (adeno-associated virus-like particles) as novel mimotope carriers. Furthermore the potential inhibitory effects of an AAVLP tumor vaccine against tumor growth should be tested.

AAV (adeno-associated virus) is a non-human pathogenic, replication defective ssDNA virus, consisting of 60 copies of three similar capsid proteins. Fusion proteins of mimotope and a capsid protein can be assembled as virus-like particles, AAVLPs. AAVLPs present the mimotope 60 times on the particle surface in a high density display fashion.

In this study first the immunogenicity, specificity and safety aspects of an AAVLP mimotope vaccine was evaluated using an ovalbumin B-cell epitope as a model antigen. Next, the specific anti – tumor effect induced by an HER-2 mimotope vaccine in AAV formal was tested in a BALB/c tumor transplant mouse model.

1 Introduction

1.1 Cancer

The immune system is responsible for keeping body homeostasis by protection against invading pathogens and by elimination of self- cells, which are suspicious due to modified surface, characteristics and growth. Tumor cells break basic rules of cell behavior, as they show uncontrolled growth by increased cell division rate, often accompanied by decreased apoptosis besides other aberrant characteristics.
Together, this gives rise to a neoplasm, which in the beginning is benign, as long as the basal lamina stays intact and therefore does not infiltrate other tissues or the vascular system. A neoplasm in that stage has a better prognosis than a tumor, having penetrated the basal lamina. Local destructive growth and/or invasiveness are the main characteristics of cancer. When the basal lamina is destroyed, the malignant cells may invade surrounding tissues and penetrate blood and lymphatic vessels. Disseminated tumor cells may form secondary tumors called metastases, which may severely harm also distant organ functions of the cancer patient, illustrated in figure 1.1.

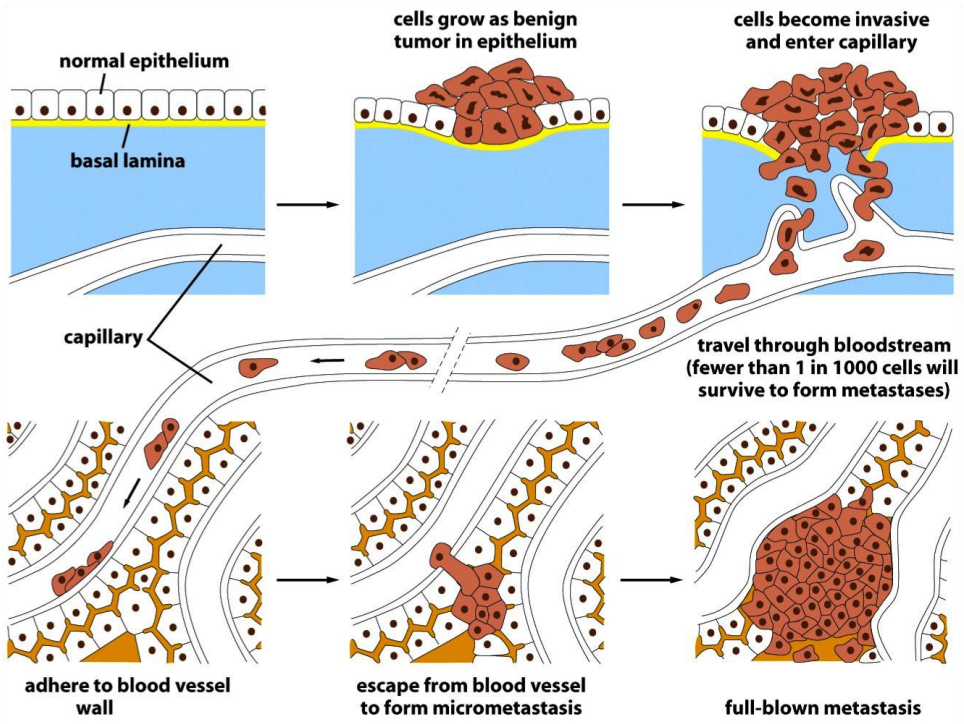

Figure 1.1: Way of metastasis from Alberts et al. [1].

Tumors can be classified according to their original cell type or tissue location, e.g. a tumor originating from connective tissue or from muscle cells is defined as sarcoma.

A tumor with epithelial origin is called carcinoma, which is the most common form of cancer in humans. About 80% of tumors are originating from epithelial tissue, which is often related to a) exposure of internal or external body surfaces to physical or chemical environmental stress causing genotoxic events, and b) intrinsically higher proliferation rate reducing the time for successful DNA-repair, and a risk to amplify mutated cells.

Tumors are further classified according to the benignity or malignity. For instance an adenoma is a benign epithelial tumor with glandular organization, whereas adenocarcinoma is its malign form. There are many other categories of tumors like leukemia, lymphoma, glioblastoma, etc. depending on the cell type and origin [1].

In figure 1.2 worldwide cancer incidence and mortality of the year 2008 is illustrated. The most frequently occurring tumors in both sexes are found in the reproductive tract, in the respiratory system and in digestive organs. Breast cancer is the leading type of tumors in the female population worldwide [2].

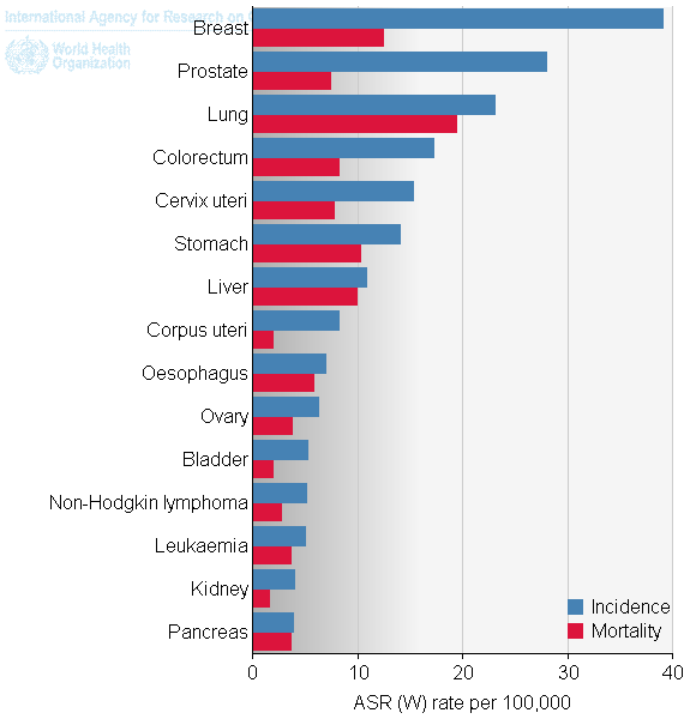

Figure 1.2: GLOBOCAN worldwide cancer incidence and mortality in women and men [2].

1.2 Breast cancer

Breast cancer is a malignant neoplasm originating from breast tissue, called mammary carcinoma and is one of the most malignant and common forms of female cancer [3].

1.2.1 **Epidemiology: Mortality and Morbidity**

The lifetime risk for mammary carcinoma in females is up to one tenth. Mammary carcinoma comprises 16% of all female tumors and about 11% of all breast cancer patients are young women at the age below 35 [3,4]. In western societies breast cancer shows the highest incidence rates which has been correlated to modern life style, as outlined below. Incidence is lower in less-developed countries due to higher rates of infectious diseases possibly triggering immune responses and lower overall expectancy of life [5].

According to the GLOBOCAN World Cancer Report of the year 2008, breast cancer was the cause of 458.503 deaths worldwide, comprising about 13.7% of all female cancer deaths [2]. Mammary carcinoma is 100 times more common in women than in men, although males tend to have poorer outcomes due to delayed diagnosis [6].

1.2.2 **Physiology and Pathology**

1.2.2.1 ***Anatomy and Physiology***

The female breast, also called *mamma* (lat.) consists mainly of the mammary gland, as well as adipose and connective tissue, anatomically located on the muscle *musculus pectoralis major*. The mammary gland consists of 10 to 20 smaller single glands called *Lobi* with one major *ductus lactifer colligens,* ending in the *sinus lactifer* located in the *mamilla*, responsible for secreting milk. Blood supply is performed mainly by the internal mammary artery and venous drainage by the axillary vein. Anatomy of the female breast is illustrated in Figure 1.3 [7].

1	thorax
2	musculus pectoralis major
3	lobi
4	mamilla
5	areola
6	ductus lactifer colligens
7	adipose tissue
8	skin

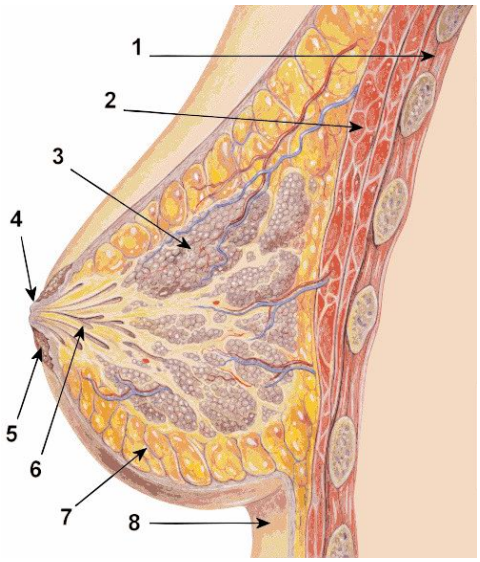

Figure 1.3: Anatomy of female breast [8].

1.2.2.2 ***Pathology***

Tumors may often be etiologically related to previous inflammations of the mamma, defined as mastitis. Mastitis often is very painful and of bacterial or viral origin resulting during breast-feeding.

Fibrous cystic mastopathia is a proliferation of connective tissue forming cysts followed by nodular lesions. In some cases epithelia start to proliferate very quickly and atypically, which may be an indication for tumor initiation.

A fibroadenoma is a benign neoplasm, very robust and compact with a clear borderline, originating from proliferation of connective tissue and glands, often diagnosed in young women aged around 20. Other benign tumors of the mamma are intraductal papillomas and phylloid tumors [9].

Breast cancer malignancies can be classified in different ways. According to the histopathology most breast malignancies arise from epithelia of a duct or a lobule, consequently called ductal or lobular carcinoma. If the basal membrane is still intact and the tumor has not yet infiltrated other tissues, tumors are described as lobular carcinoma in situ (LCIS) or as ductal carcinoma in situ (DCIS). According to Nottingham Modification of the Bloom-Richardson grading another indication is that surrounding tissue is still untouched and tumor progression is of low grade. This grading system categorizes tumor cells according to their differentiation, meaning their tubule formation, nuclear pleomorphism and their mitotic counts. Well-differentiated cells are classified as low grade (grade 1), intermediate differentiated as grade 2, poorly differentiated (or high grade) cells as grade 3 and undifferentiated, finally the highest grade (grade 4) is associated with poorest prognosis [9].

The TNM classification of malignant tumors has been developed by the Union for International Cancer Control (UICC) and the American Joint Committee on Cancer Staging (AJCC). T stands for the size of the Tumor, N defines whether regional lymph Nodes are affected, and M describes whether a tumor has already Metastasized. Together, T, N and M are used for tumor staging I to IV. Stage 0 is defined as pre-cancerous condition, i.e. tumor in situ (Tis) either a DCIS or a LCIS; stage I to III means cancer without metastasis and relatively good prognosis and stage IV classifies advanced metastatic carcinoma with poor prognosis (table 1.1) [10].

T (CIS, 0–4): T0: no primary tumor
T1: primary tumor smaller than 2cm
T2: primary tumor 2 – 5cm
T3: primary tumor bigger than 5cm

N (0–3): N0: no tumor cells in regional lymph nodes
N1: metastasis present in regional lymph node
N2: tumor spread between N1 and N3
N3: tumor cells in distant or numerous regional lymph nodes

M (0/1): M0: no distant metastasis
M1: metastasis in distant organs (beyond regional lymph nodes)

Table 2. TNM Stage Grouping for Breast Cancer

Stage Grouping			
0	Tis	N0	M0
I	T1*	N0	M0
IIA	T0	N1	M0
	T1*	N1	M0
	T2	N0	M0
IIB	T2	N1	M0
	T3	N0	M0
IIIA	T0	N2	M0
	T1*	N2	M0
	T2	N2	M0
	T3	N1	M0
	T3	N2	M0
IIIB	T4	N0	M0
	T4	N1	M0
	T4	N2	M0
IIIC	Any T	N3	M0
IV	Any T	Any N	M1

Table 1.1: TNM staging for breast cancer [10].

1.2.3 **Etiology of breast cancer**

Different risk factors that induce tumor initiation could be identified, like age and sex [4,6]. Especially high levels of estrogen play a major role in breast cancer etiology, like early menarche, late or lack of childbearing or breastfeeding and late menopause [11]. More recently, also contraceptives and hormone replacement during menopause were discussed as possible factors. Higher incidence in the western world, like North America, Western and Northern Europe and Australia correlates with higher income and modern lifestyle, associated with high alcohol consumption, tobacco smoking, high fat diet and obesity. All of these aspects have been associated with the risk of tumor formation in the female breast, compared to much lower incidence values in lower family income countries [12-14].

Moreover, breast cancer can be the result of genotoxic events. DNA damages caused by UV-radiation or other environmental factors are usually corrected by special DNA repair programs. These DNA repair mechanisms can be overwhelmed when the number of genotoxic events increase. Mutations are especially critical when occurring in gene loci coding for tumor suppressor proteins or proto-oncogenes. Mutation in

these genes can result in loss-of-function of proteins having significant regulatory functional on cell growth and often may lead to carcinogenesis. One of the most common mutations associated with breast cancer is observed in the gene BRCA1 (breast cancer antigen 1) that is mainly responsible for DNA repair of double strand breaks. The gene BRCA1 is located on the long arm of chromosome 17 at band 21 and a loss-of-function of this protein increases the risk for breast cancer as part of the hereditary breast-ovarian cancer syndrome [15]. Similar effects result from BRCA2, located on the long arm of chromosome 13 at position 12.3, which also interacts in DNA repair of double strand breaks [16]. It could also be demonstrated that 5 to 10% of all breast cancers are hereditary; 80 to 90% of those are caused by mutations in the genes BRCA1 or BRCA2 [17].

1.2.4 **Diagnosis**

Early symptoms, like suspicious nodes should be taken seriously, although luckily in many cases they turn out to be unrelated to breast cancer. Also atypical locations, like a node beneath the breast, in the axilla or in supraclavicular areas can be hints for breast cancer, as well as pain, ulceration, skin dimpling, skin discoloring, edema, erythema or inversion of the mamilla. For screening purposes, mammograms should be carried out every second year after the age of 40 and even more often in high-risk families. Nodes, calcifications or other pathologic alterations can be detected by a mammogram and are an indication for further diagnostic procedures, like histological and cytological core biopsies or abdominal sonographies [18,19].

For choosing the right treatment and prediction of prognosis, definition of the receptor status on the surface of tumor cells is essential. There are three major tumor associated antigens that can be expressed on the surface of mammary carcinoma cells: estrogen receptor (ER), progesterone receptor (PR) and human epidermal growth factor receptor 2 (HER-2). ER and PR can be stimulated by the respective hormones with positive effects on tumor growth. These tumors are often associated with relatively better prognosis. HER-2 expression, however, correlates with bad prognosis. The present Master thesis concentrates on this important molecule. Tumor cells with none of these receptors expressed on their surface are defined as basal-like or triple negative [20].

1.2.5 **Human Epidermal growth factor Receptor 2**

The Human Epidermal growth factor Receptor 2 (HER-2, HER-2/neu, ErbB-2, c-erbB-2, p185HER-2) is a 185kDa protein [21]. The HER-2 proto-oncogene is located on chromosome 17q21 and encodes 1255 amino acids forming the transmembrane glycoprotein p185HER-2 or simplified the HER-2. HER-2 belongs to the family of epidermal growth factor receptors (EGFR family). As the other family members, HER-1 (ErbB-1), HER-3 (ERbB-3) and HER-4 (ErbB-4), HER-2 is a transmembrane tyrosine kinase receptor. All except HER-3 harbor functional intracellular tyrosine kinase domains and a transmembranous lipophilic segment. All members of the EGFR family, except HER-2, additionally possess an extracellular ligand-binding domain [22].

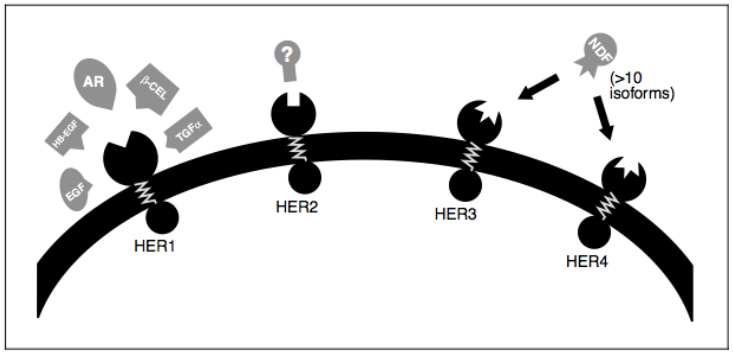

Figure 1.4: Ligands binding to HER family members [23].

As illustrated in figure 1.4, selected ligands that trigger the EGFR family members are the epidermal growth factor (EGF), transforming growth factor - α (TGF-α), amphiregulin (AR), heparin-binding EGF (HB-EGF), neurigulins (NRG), epiregulin (EPR). The single EGFR family members must dimerize to become activated. They form either heterodimers or homodimers which activate by cross-phosphorylation the Ras-MAP-Kinase signaling pathway or the PI3-Kinase signaling machinery, consequently stimulating cell proliferation, cell survival, cell mobility and neoangiogenesis via VEGF release (figure 1.5). However HER-2 is the preferred signaling partner chosen by all other isoforms [22-24].

To shut off signaling EGFR complexes are internalized via clathrin-coated pits and transported to the endosome, where ligands are removed and degraded and free receptors can be shuttled back to the cell membrane. Moreover, the receptors can be degraded as well, whereby the adaptor protein Cbl, an ubiquitin ligase, plays a prominent role.

Also anti-HER2 antibodies induce degradation and thus down regulation of HER-2 by recruiting Cbl [23,24].

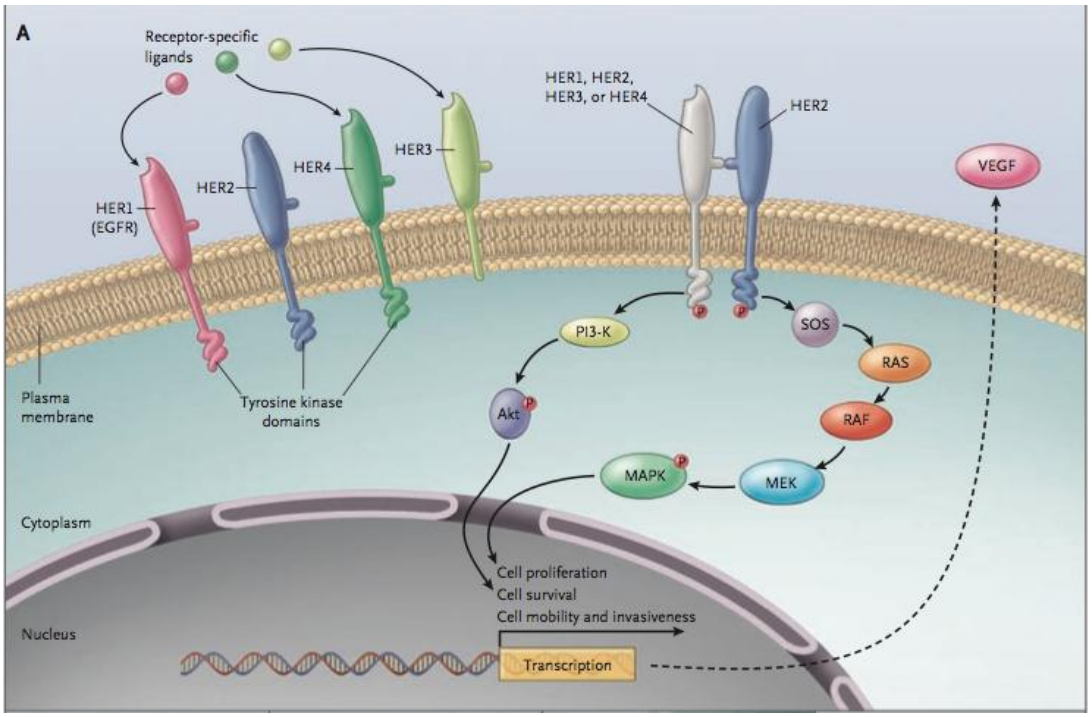

Figure 1.5: EGFR family members and signaling [22].

In physiological condition HER-2 and the other EGFR family members play a prominent role in the development of the human fetus, especially of the nervous system, developing of bone, muscle, skin, heart, lungs and intestinal epithelium. In contrast, only low levels of these proteins are expressed in mature tissue. In settings of HER-2 overexpression growth signaling cannot be shut off, meaning enhanced cell multiplication and survival causing malignant growth and tumor formation. Furthermore, degradation of the receptor is impaired, leading to recycling back to the plasma membrane, making them available for a new signal stimulus. The monoclonal antibody trastuzumab (Herceptin®), targeting HER-2, interferes in this potent and aggressive mechanism, which will be discussed below. Consequently, reduced numbers of HER-2 molecules are no longer available to form heterodimers with other HER family members, thus minimizing signaling and alleviating tumor growth [22-24].

1.2.6 **Therapies against breast cancer**

According to the stage of disease, different therapy options are available including combinations of surgery, chemotherapy, anti-hormone treatments or irradiation [18].

Localization of the tumor, inflammation, whether there is a clear borderline between tumor and breast, and the age of the patient are important factors to decide if only a part or the whole breast will be removed. Today, the overall aim is to operate breast-conservingly, especially in young patients. Nevertheless it is important to remove tumor tissue along with surrounding healthy tissue and to check for proximate lymph nodes in the axilla, especially the sentinel lymph node, which is the first draining lymph node of the tumor region. Hence cryosections from breast tissue and lymph nodes are taken during the surgical intervention and checked for affection [25].

Often after surgery radiotherapy is used to destroy remnants of tumor cells that could not be removed surgically and may proliferate or invade damaged tissue caused by surgical wounding. Furthermore it alters the tumor microenvironment making it less favorable for tumor cell growth and invasion. Radiotherapy can additionally be given intra-operatively, which results in relatively higher tumoricidal effects than conventional whole-breast radiotherapy [26].

Hormone blocking therapies are applied in hormone receptor positive breast cancer, e.g. ER positive. Estrogen is a growth stimulus for tumor proliferation and can either be treated by inhibition of the hormone receptor, or with drugs that block the effects induced by the hormone. Alternate hormone therapy agents are aromatase inhibitors which inhibit the production of estrogen in women [27].

The mechanism of chemotherapy most often applied intravenously is to destroy fast growing cells, which replicate more often, a main characteristic of many cancer cells. Another mechanism is induction of DNA damage resulting in cell death. The main problem of chemotherapeutics is their high systemic toxicity, meaning that they unspecifically kill dividing cells, including cells in bone marrow, the digestive tract and hair follicles, resulting in massive side effects. The most commonly used chemotherapeutics are Cyclophosphamid, Epidoxorubicin and 5-Fluorouracil (CEF-scheme). This combination especially bears a high risk of cardiotoxicity [28].

All these above mentioned therapy options for cancer treatment produce either local or systemic serious side effects, which can be avoided with targeted therapy, for instance by using monoclonal antibodies. These antibodies are derived from a specific B-lymphocyte clone detecting one specific epitope. In contrast, polyclonal antibodies are derived from different B-cell clones recognizing each a different epitope of a specific antigen [29].

1.2.7 **Trastzuzmab (Herceptin®)**

The most prominent monoclonal antibody with clinical activity against HER-2 overexpressing mammary carcinoma cells is trastuzumab (Herceptin®). The U.S. Food and Drug administration (FDA) approved it for passive immunotherapy for metastatic breast cancer in the year 1998. Trastuzumab is the basis for all our immunotherapeutical approaches against cancer [30]. Figure 1.6 illustrates the antibody – HER-2 complex.

A

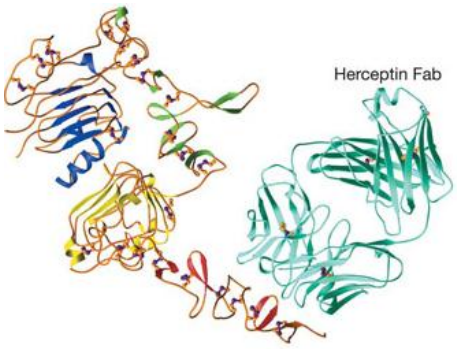

B

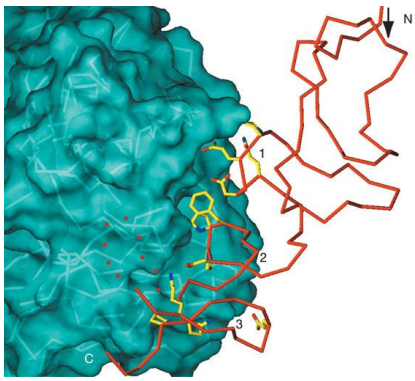

Figure 1.6: A) 3D-model based on co-crysalization of trastuzumab binding to HER-2.
The different domains of HER-2 are colored in blue (domain I), green (domain II), yellow (domain III) and the domain IV in red. Purple and gold show disulphide bonds of the molecules. Herceptin is colored in turquoise binding to the domain IV [31].

B) Detailled molecular analysis of the trastuzumab epitope on HER-2.
The figure shows the exact attachment of trastuzumab to sHER-2. Herceptin® is again colored in turquoise and the backbone domain IV of HER-2 in red. Yellow demonstrates the side chains of residues contacting the Fab region of the humanized antibody. The N and C termini of the displayed HER-2 region are indicated as three loop regions, loop 1 (residues 557–561), loop 2 (residues 570–573) and loop 3 (residues 593–603), which are in contact to the Herceptin Fab fragment. Red dots indicate an eight-residue loop not directly visible in the structure [31].

Trastuzumab is a humanized antibody, being constructed of human variable region framework residues and an IgG1 constant domain, but still containing the antigen binding loops from the original mouse monoclonal antibody 4D5 [32].

There are several described mechanisms of action of this antibody, illustrated in figure 1.7. One way is that trastuzumab binds a juxtamembrane domain of the extracellular part of HER-2 to prevent signaling induced by the membrane-bound-phosphorylated protein p95, a HER-2 fragment emerging from cleaving (C). Furthermore, trastuzumab can block either homo- or heterodimerization of HER-2 with other members of the EGFR family, which favors dimerization of the other HER members resulting in minimization of the tumor promoting signals (D). Trastuzumab may interact via its Fcγ domain with FcγR positive effector cells, such as NK cells and induce antibody-dependent cell-mediated cytotoxicity (ADCC) (E). Finally, trastuzumab induces vesicular endocytosis resulting in HER-2 degradation leading to receptor down-regulation and making the cancer cells less susceptible to growth stimuli (F).

To sum up, trastuzumab binds HER-2 and thereby inhibits its signaling cascade, resulting in inhibition of tumor growth, proliferation, lower cell survival and inhibition of invasiveness [22,30].

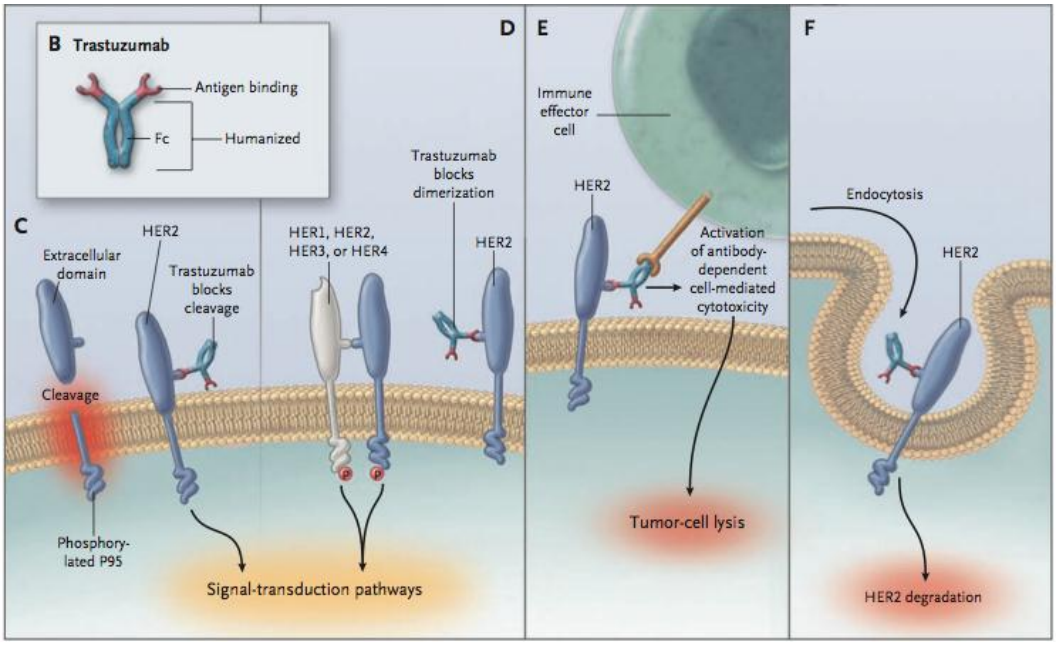

Figure 1.7: Herceptin® activity mechanism [22].

Trastuzumab can be used alone or as an adjuvant to almost all conventional chemotherapies for treatment of HER-2 overexpressing breast cancers being above 2+ or 3+ using the HercepTest® in immunohistochemistry or the FISH (Fluorescence In Situ Hybridization) technology. According to a patient's indication, contraindication

and coexisting conditions, a loading dose of 4-8mg, followed by 6mg per kg body weight every third week is recommended. The advantage of this targeted therapy is to circumvent or reduce classical side effects caused by other anti-tumor treatments. Nevertheless there are still adverse reactions against the passively applied monoclonal antibody in some patients, like cardio toxic effects or acute hypersensitivity reactions, but lower amounts than 10% [21,22].
Other critical limitations of monoclonal antibody therapy are their limited half-life, prolonged application time, irregular distribution in tissue and the immense production costs to achieve sufficient antibody titers for anti-tumor activity. All these factors decrease attractiveness of the otherwise so successful passive immunotherapy. Therefore an active immunotherapy rendering antibodies of similar specificities like trastuzumab would be an interesting and promising treatment alternative, with the advantage of a continuously available polyclonal immune response, taking advantage of effector mechanisms of several immunoglobulin isotypes [33-35].

1.3 Mimotopes

Mimotopes are small epitope-mimicking structures, varying from 6 to 20 amino acids in length. Mimotopes thus harbor equivalent structural, biological and physicochemical properties and only sometimes a similar sequence as their natural epitope on an antigen. Yet sequence homology alone is not enough to resemble a conformational B-cell epitope and therefore, is not really necessary. Mimotopes very closely, but not completely, resemble the 3D-structure of the original epitope, with its biochemical and electrostatic properties. When used for immunization, mimotopes induce similar antibody specificities as the natural antigen epitopes, due to the principle of molecular mimicry.

This mechanism can be exploited in anti-cancer therapy. When tumor cells overexpress tumor-associated antigens (TAA), e.g. growth factor receptors or glycoproteins, they are by nature well-tolerated self-molecules of low antigenicity. Via the mimotope technology it is possible to generate epitope mimics which are similar, but not identical to the TAA. These TAA mimotopes are therefore suitable to break tolerance and to induce a B-cell epitope-specific humoral immune response with memory function. Antibodies produced by mimotope vaccination are therefore not only directed against the immunogen, but also towards the natural epitope expressed on the tumor cell. This polyclonal antibody response composed of different immunoglobulin isotypes with various effector functions can consequently stimulate

ADCC, complement-dependent cytotoxicity (CDC) and other effects resulting in cancer cell death, depicted in figure 1.8 [35,36].

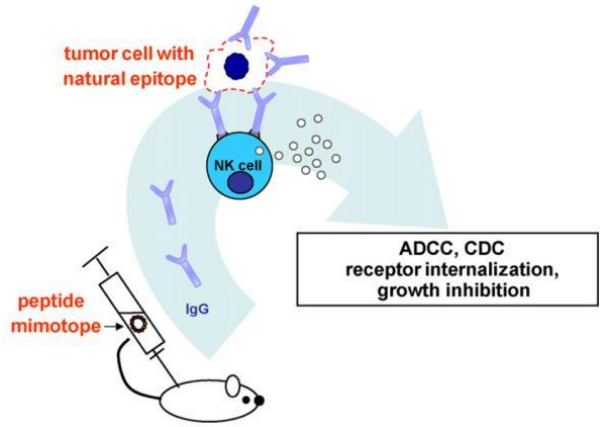

Figure 1.8: Mimotope vaccines: Epitope mimics induce anti-cancer antibodies. Due to molecular mimicry, mimotope vaccines induce a polyclonal immune response not only directed against the mimotope, but also against the natural tumor-associated antigen. These antibodies are able to mediate cytotoxicity in cancer cells, like ADCC or CDC [36].

Antibodies can be tumor-inhibitory or tumor-promoting due to their epitope specificity. The latter would eventually even enhance malignant growth (figure 1.9). Thus the definition of the epitope-specific biological function of antibodies and the definition of the exact molecular binding site is of fundamental importance. Hence, the identification of reactive centers, ligand-binding grooves, as well as crystallization experiments of TAAs are of considerable importance for the directed induction of growth inhibitory immune responses [33,37].

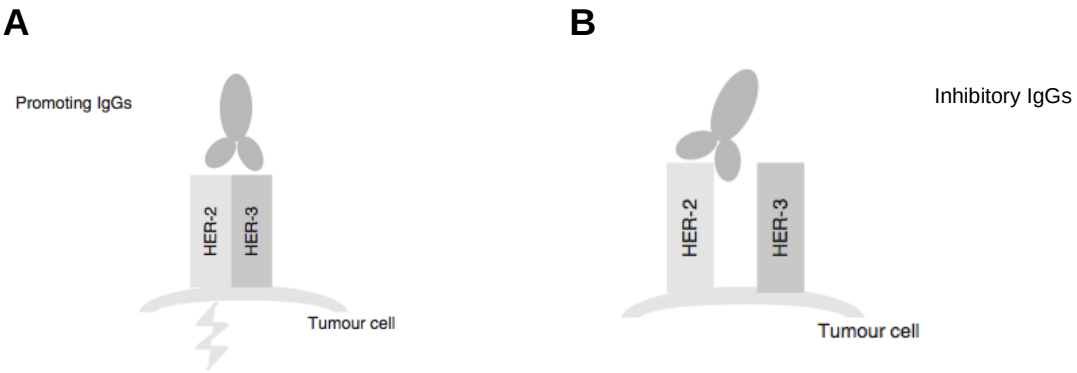

Figure 1.9: Promoting (A) and inhibitory (B) antibodies. Heterodimerization of HER family members induced by IgG antibodies promotes strong signaling in cancers (A); in contrast, inhibitory IgGs block heterodimerization resulting in down regulation of tumor promoting signals (B) [35].

Having determined mimotopes for the natural epitope, synthetic peptides can easily be produced. They are chemically stable, cost-effective and do not contain any infectious, toxic or oncogenic materials. However, due to their small size they are haptens only and non-immunogenic. To act as complete antigens and immunogens they have to be bound to a carrier molecule. Then, they can induce tumor-targeting antibodies. This could be demonstrated in a previous study for HER-2 mimotopes by our group. In this approach, we generated mimotopes by using the monoclonal antibody trastuzumab for screening a phage display peptide library [34].

1.3.1 **Phage display technology**

Phage display library screening as a technology for generating mimotopes was first described in 1985 [35]. Phage libraries display about 10^9 or more different peptides. The colony repertoire is generated by cloning oligonucleotides into the genome of a phage, e.g. the filamentous bacteriophage fd using either minor (pIII) or major (pVIII) phage coat protein for surface display. Peptides can be presented in linear or in circular form, their length may vary between 6 to 38 amino acids in the different libraries.

In the so called “biopanning” procedure, typically antigen specific antibodies are absorbed onto microtiter plates and incubated with the phage display peptide library. Antibodies will absorb then phages displaying peptides similar to the original epitope, whereas other phages are washed away during the following washing steps. Specifically bound phages are eluted by pH-change or by competition with the natural antigen and amplified for a next selection round. By several biopanning rounds, binding phage clones can be highly enriched. Subsequent colony screening methods identify the most specifically interacting phages, which are then cloned and sequenced.

Selected mimotopes have to be stringently tested for specificity, mimicry and immunogenicity, illustrated in figure 1.10 [35].

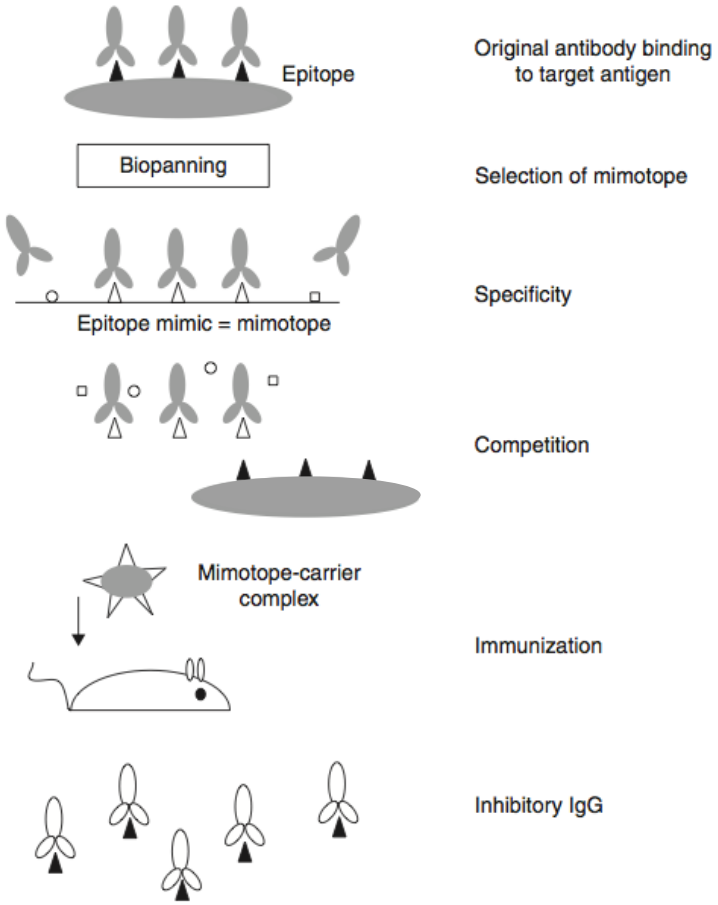

Figure 1.10: In “biopanning”, specific mimotopes are selected by incubation with a monoclonal antibody. After several rounds to enrich the number of binding phages, mimotopes were tested for specificity, mimicry and immunogenicity [35].

1.3.2 **Mimotope carrier**

As already mentioned above mimotopes have to be coupled to carriers before vaccination.

KLH (keyhole limpet hemocyanin) is a typical carrier, being even FDA approved. It is a large multi subunit, oxygen-carrying glycosylated metalloprotein, derived from the hemolymph of the giant keyhole limpet. KLH elicits strong immune responses by offering additional T-helper epitopes for stimulating B-cells. Additionally KLH may activate cytotoxic T-cells (CTL) by inducing the production of interleukin IL-2 [35,38].

Another example of a system to achieve high antigenic density are MAPs (multiple antigenic peptides). Thereby, linear peptides are synthesized directly on a tyrosine backbone in tetrameric or octameric form. In studies with CEA (carcino embryonic antigen) - mimotopes an octameric “multiple antigen mimotope” (MAM), was successfully employed in preclinical anti-cancer vaccination studies [35,38].

Many different carrier technologies are currently in development, including viral and bacterial vectors (DNA vaccines), liposomes, ISCOMs (immune stimulating complexes, based on lipids), micro- and nanoparticles and others. However, virosomes and virus-like particles are regarded as the most promising technologies for vaccine antigen delivery today. Both, virosomes and VLPs make B-cell epitopes of interest highly immunogenic [39,40].

Considering the fact that vaccination originally was developed and employed most successfully in infectious diseases, also we hypothesized that virus particle might be attractive carrier systems for mimotopes. In this master thesis we propose Adeno-associated viruses as an ideal carrier platform for B-cell epitopes, i.e. mimotopes.

1.3.3 **Adeno-associated virus**

Adeno – associated viruses (AAV) are nonenveloped small ssDNA viruses and belong to the Baltimore classification type II viruses, illustrated in figure 1.11. They are also members of the genus *Dependoviruses* from the family *Parvoviridae*. AAVs are replication defective, meaning that they are not able to replicate without a helper virus, which is in this case an Adenovirus (AV). Although AAVs are nonpathogenic to humans, they can infect dividing and non-dividing cells, and furthermore they are able to integrate latently into host DNA, resulting in seropositive individuals [41,42].

A

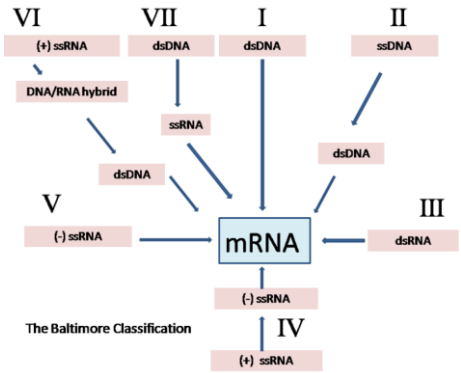

B

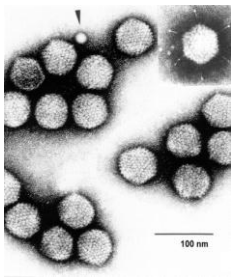

Figure 1.11: Baltimore classification (A) and electron microscopy of AAV (B) [43].

12 different primate serotypes (AAV1-12) exist with icosahedral symmetry. AAV2 consists of 60 capsomers, each a quadrilateral 'kite-shaped' wedge, which allows the incorporation of a selected antigen or protein for display on the particle's surface, as can be seen in figure 1.12. A protein of interest, an epitope or a mimotope can be

displayed thus 60 times on the surface of the capsomeres by modifying the gene sequence of the AAV.

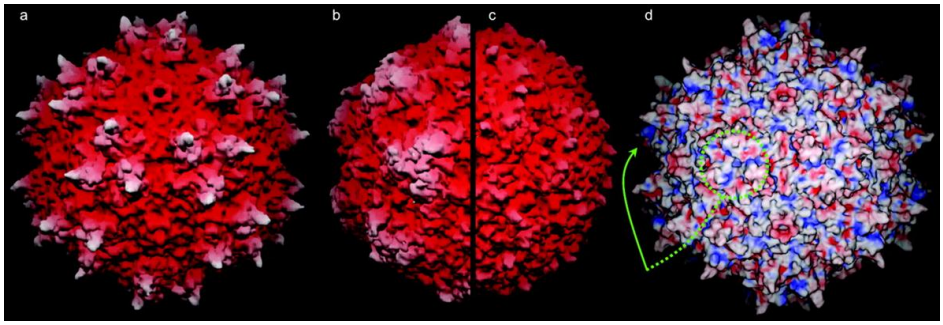

Figure 1.12: Atomic structure of adeno-associated virus (AAV2) [41].

AAVs enter cells via binding to heparan sulfate proteoglycan, the primary cellular receptor binding of this virus. Furthermore, co-receptors like fibroblast growth factor receptor-1, hepatocyte growth factor receptor and αvβ5 integrin are involved in the internalization program of AAV2. After docking for cell entry, viruses are taken up by receptor-mediated endocytosis through clathrin-coated pits and get transported to the nucleus by different possible pathways, depicted in figure 1.13. The virions are processed in the endosome. Consequently a phospholipase domain located on the capsid allows endosomal escape and nuclear targeting. In the nucleus uncoating is performed, releasing the viral genome for integration into the host cell genome or to form episomes [44-46].

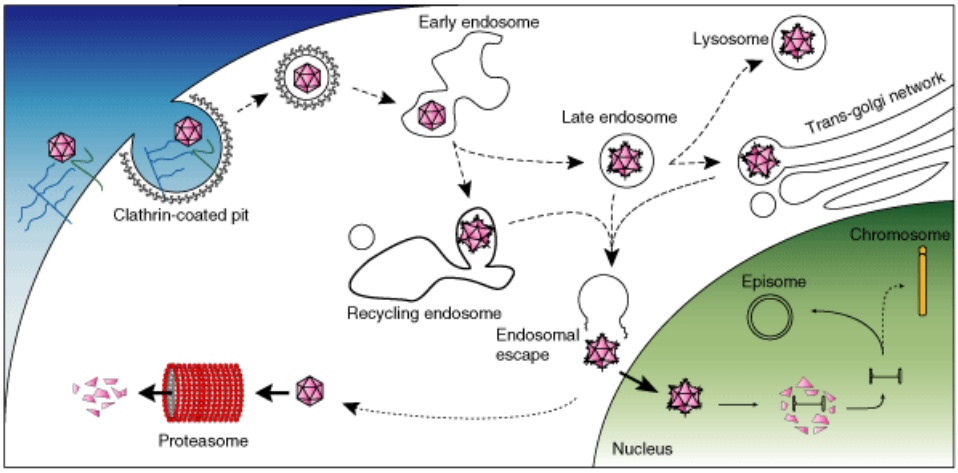

Figure 1.13: rAAV2 cell entry and life cycle [44].

1.3.4 **Adeno-associated virus like particles**

Vaccination with viruses, although often in attenuated or inactivated form, elicits strong immune responses but may induce several side effects. These difficulties can be solved by recombinant techniques, which allow the production of simple viral structures or capsids lacking viral nucleic acid and therefore minimizing virus induced disadvantages [40,47].

Adeno-associated virus-like particles (AAVLP) are generated synthetically via assembling of only one backbone capsid protein, which in this master thesis is VP3. A B-cell epitope of choice can be fused into appropriate insertion sites of VP3 in order to enable high-density presentation on the surface of assembled VLP [48]. By definition AAVLPs do not carry any DNA as they assembled without any genetic material. AAVLPs are of general viral size, but exact size and morphology depends on the nature of the epitopes, engineered into the VP3 fusion protein. The assembled VLP represents a more immunogenic tool than single subunits of proteins and stimulate the humoral as well cellular immune responses. Yet, VLPs do not induce an immune reaction as strong as conventional viral vaccines, immunization therefore requires frequent and larger doses in combination with a dominant adjuvant. Besides presentation of the chosen protein VLPs also mimic the structure of the native virus resulting in the formation of antibodies. Some VLPs via uptake by dendritic cells and presentation across MHC class II show self-adjuvant effects, meaning stimulation of the innate immune system. However, also CTLs can be activated by exogenous VLPs that were cross-presented by MHC class I molecules. Simultaneous activation of the innate and adaptive branches of the immune system is thus another advantage of VLP vaccines. In addition, they are a safe and effective approach for triggering antibody production against surface epitopes in cases where soluble forms of proteins fail to be sufficiently effective (figure 1.14) [49].

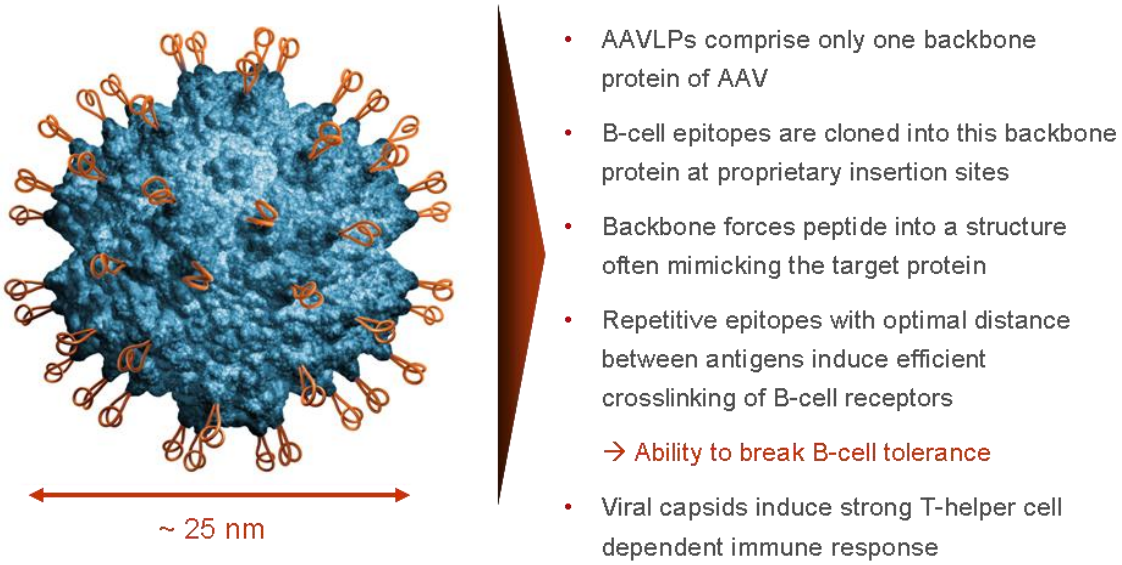

Figure 1.14: Key facts of AAVLPs as vaccine display system [50].

1.3.5 **Adjuvants**

Adjuvants are tools to enhance the immune responses toward vaccine antigens to induce high levels of antibodies and T-cell responses. Further they may modulate the resulting immune response and support memory function. Another advantage is that less antigen and fewer injections are needed when adjuvants are used due to depot effects. There are different adjuvants available (reviewed by our group in [51]) among which the most prominent were selected for experiments within this master thesis and are shortly discussed below:

A) The adjuvant aluminum hydroxide (Alum) is the most widely used adjuvant. It absorbs antigens via electrostatic, hydrophobic attraction and ligand exchange. Alum enhances the efficacy and duration of antigen presentation by antigen presenting cells (APCs) by forming a depot at the site of injection and thus high and sustained local antigen concentration. Among APCs, activated macrophages adapt a dendritic cell-like phenotype that further stimulates T-cells, especially T_H2 cells, releasing IL-4 causing isotype switch towards IgG1 and IgE in mice. Although Alum is broadly and successfully used in a plethora of vaccines, including allergen immunotherapy, its usage might be a disadvantage in treatment of allergy due to further boost of T_H2 bias. Side effects may in rare cases be granuloma formation, abscesses, eosinophilia or myofasciitis, but overall aluminum hydroxide is regarded as safe and accordingly is also FDA approved [51].

B) The other adjuvant used exemplarily in this study is Montanide ISA adjuvant®, a water-in-oil emulsion based on a lipid formula. It consists of an enriched light mineral

oil extremely emulsified with mannitol and purified oleic acid of vegetable origin. Montanide favors humoral immunity without cell-mediated response. Adverse reactions may be abscesses and granuloma formation, which could be minimized by decreasing the amount of injection [52,53].

1.4 Allergy

1.4.1 **Hypersensitivity reactions**

Hypersensitivity or allergy defines a condition where adaptive immune responses are triggered against non-harmful environmental antigens, such as food, pollen or drugs. According to the Coombs and Gell classification, allergy can be classified into four types, type I to type IV (illustrated in figure 1.18). Type I hypersensitivities are immediate reactions mediated by IgE antibodies and are directed against soluble antigens, termed allergens. Upon exposure to an allergen susceptible individuals may get sensitized and form IgE, which immediately gets fixed to high affinity IgE receptors on inflammatory cells such as mast cells or basophile granulocytes. Upon subsequent allergen encounter, the allergen can then crosslink IgE on effector cells in diverse tissues, resulting in mediator release. The most important mediator is histamine, rendering vasodilatation and bronchoconstriction, leading to the clinical symptoms of e.g. asthma, allergic rhinitis or systemic anaphylaxis within minutes.

Type II allergy reaction is mediated by IgG antibodies that bind to cell-surface or matrix-associated antigens recognized by phagocytes. Target cell destruction may then be initiated by immune complex mediated complement activation. Examples of this kind of hypersensitivity reaction are drug allergies or rhesus incompatibility, where a Rhesus negative mother (sensitized during a first pregnancy) gives birth to a second Rhesus positive child. Then maternal IgGs are directed against the rhesus antigen on fetal erythrocytes, which may lead to severe hemolysis (morbus heamolyticus neonatorum).

In type III hypersensitivity, IgG antibodies are formed against soluble antigens rendering immune complexes additionally activating the complement system. These formed immune complexes precipitate, cause inflammation in e.g. endothelia, skin or intestine and are able to trigger tissue damage. The two major types of type III reaction are Arthus reaction and serum sickness.

Type IV hypersensitivity reactions are T-cell mediated and delayed. They can be divided into three groups dependent on the involved T-cell type. T_H1 cells cause upon antigen contact inflammatory response by macrophage activation, like for instance in contact dermatitis or the tuberculin reaction. T_H2 cells are induced upon chronic

allergen encounter and activate predominantly eosinophils. Eosinophilic inflammation is typically seen in chronic asthma or chronic allergic rhinitis. The third form of type IV hypersensitivity depends on cytotoxic T-cells. This kind of inflammation is besides T_H1 cells seen in contact dermatitis [29].

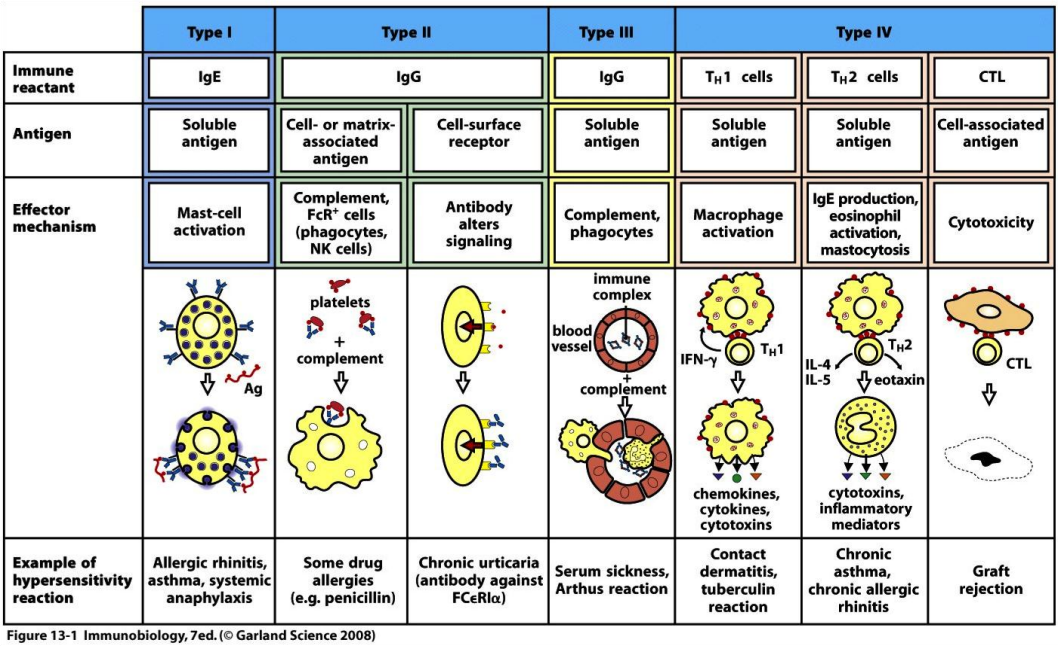

Figure 1.15: Coombs and Gell classification of hypersensitivity [29].

1.4.2 **Ovalbumin as model antigen/ allergen**

Ovalbumin (OVA) is the main component of a bird's egg white, making up about 60 to 65% of the total proteins in egg. It is a glycoprotein with relative molecular mass of 45 kDa and it is built up of 385 amino acids. Ovalbumin belongs to the family of the serpins, but lacks serine protease inhibitor activity. The protein is a strong antigen and allergen in humans as well as in animals. Therefore it is often used as model antigen/allergen in immunology and allergology. In this master study a dominant B-cell epitope of ovalbumin is used to test immunogenicity, specificity and safety aspects of the AAVLPs as novel epitope/mimotope carrier systems [54].

1.5 Aim of this study

The overall goal of this study was to test the potential of AAVLPs and AAVs as new carriers for B-cell vaccines, namely epitopes or mimotopes.

The first aim was to investigate immunogenicity, specificity, and especially *in vitro* and *in vivo* safety using a B-cell epitope of ovalbumin as model allergen, displayed by AAVLPs in an anaphylaxis mouse model.

The second aim was to use AAVs as specific display system of mimotopes of the important tumor antigen HER-2. Again, antigenicity, specificity and immunogenicity should be investigated and finally therapeutic potential of the vaccine proven using a tumor mouse model. From these studies it was expected to get sufficient arguments for also transferring the HER-2 mimotope vaccine into an AAVLP formal.

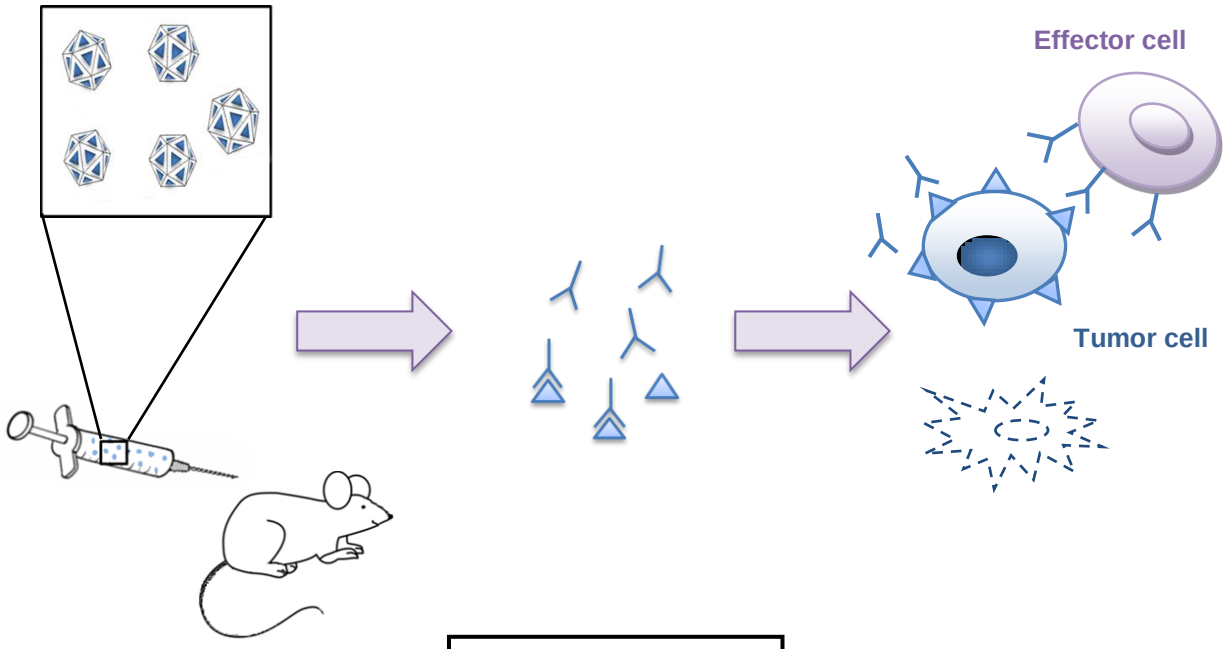

Vaccination with epitopes/ mimotopes coupled to AAVLPs

Qualitative and quantitative analysis of induced antibodies

Safety aspects of AAVLPs as carrier

Efficacy
ADCC
Tumor inhibition

Examination of specific immune response induced, by AAVLP displayed epitopes/mimotopes:

- **Immunogenicity & Specificity**
- **In vitro & in vivo Safety**
- **In vitro & in vivo Efficacy**

2 Materials and Methods

2.1 Materials

AAVLP and AAV particles suspended in 40% iodixanol were provided by Medigene (Martinsried, Germany). The adjuvant aluminium hydroxide (alhydrogel-S Suspension 1.3%, sterile) was purchased from Serva Electrophoresis (Heidelberg, Germany) and Montanide ISA 51 VG (sterile, endotoxin free) from Seppic (Cologne, Germany).
Trastuzumab (Herceptin®) and Rituximab (MabThera®) were obtained from Roche (Vienna, Austria) and Cetuximab (Erbitux®) from Merck KGaA (Vienna, Austria).
96-well flat-bottom plates were ordered from Nunc immunoplate (Roskilde, Denmark). Standard murine IgG1, IgG2a, IgG2b and IgE antibodies (BD Pharmingen, Schwechat, Austria) were used. Primary detection antibody rat-anti-mouse IgG1, IgG2a, IgG2b and IgE were purchased from Southern Biotech (Birmingham, Alabama, USA), and secondary detection antibody goat-anti-rat IgG-HRP from GE Healthcare (Freiburg, Germany). Direct HRP labelled goat-anti-mouse IgG was obtained from Abcam (Cambridge, UK). ABTS (2,2'-azino-bis 3-ethylbenzthiazoline-6-sulphonic acid) was purchased from Sigma (Vienna, Austria) and TMB substrate Reagent Set for ELISA from BD Bioscience (Schwechat, Austria).
RPMI 1640 media, IMDM media, αMEM media, DMEM/F12 media, FCS, L-glutamine, penicillin, streptomycin, G148 geneticin and sodium pyruvate were all from Gibco, (Lofer, Austria). Cell culture flasks, 75cm² with canted neck and filtered cap were used from Iwaki (Dublin, Ireland), and sterile 96-well round-bottom plates from Costar (New York, USA).
Evans blue (Merck KGaA Darmstadt, Germany). Phl p 5 (grass pollen allergen) was obtained from Biomay (Vienna, Austria). Positive mast cell degranulation compound 48/80 (40µg/mL) was purchased from Sigma (Vienna, Austria).
70 µm nylon meshes were used from BD Biosciences, Schwechat, Austria and Lympholyte-M from Cedarlane, Burlington, Canada.
Concavalin A was delivered from Sigma (Vienna, Austria).
IL-5 cytokine ELISA kit was purchased from eBioscience (Vienna, Austria).
Ni-NTA mini column Kit and Ni-NTA agarose beads were purchased from Qiagen (Hilden, Germany). Polyprep® Chromatography Columns were delivered from Bio-Rad (Vienna, Austria). Amicon Ultra-15 Centrifugal Filter Units Regenerated Cellulose 30.000 MWCO were obtained from Millipore GmbH (Vienna, Austria), Slide-A-Lyzer Dialysis Cassette 10.000 MWCO 3-5mL capacity and Pierce BCA (bicinchoninic acid) protein assay reagent both from Thermo Scientific (Fischer Scientific, Vienna, Austria).

EZ4U cell proliferation assay was used from Biomedica Group (Vienna, Austria). Protein G Sepharose 4 Fast Flow was obtained from Fischer Scientific (Vienna, Austria) and Illustra MicroSpin™ G-25 Columns from VWR International (Vienna, Austria).

2.1.1 **Particles**

AAVLPs and AAVs were constructed and provided by Medigene. Whereas for the safety study AAVLPs were provided, the HER-2 tumor mimotope experiment was less advanced and done using AAV-display. AAV clones termed DMD1, DMD2 etc. comprised different mimotope sequences which are not revealed in this diploma thesis.

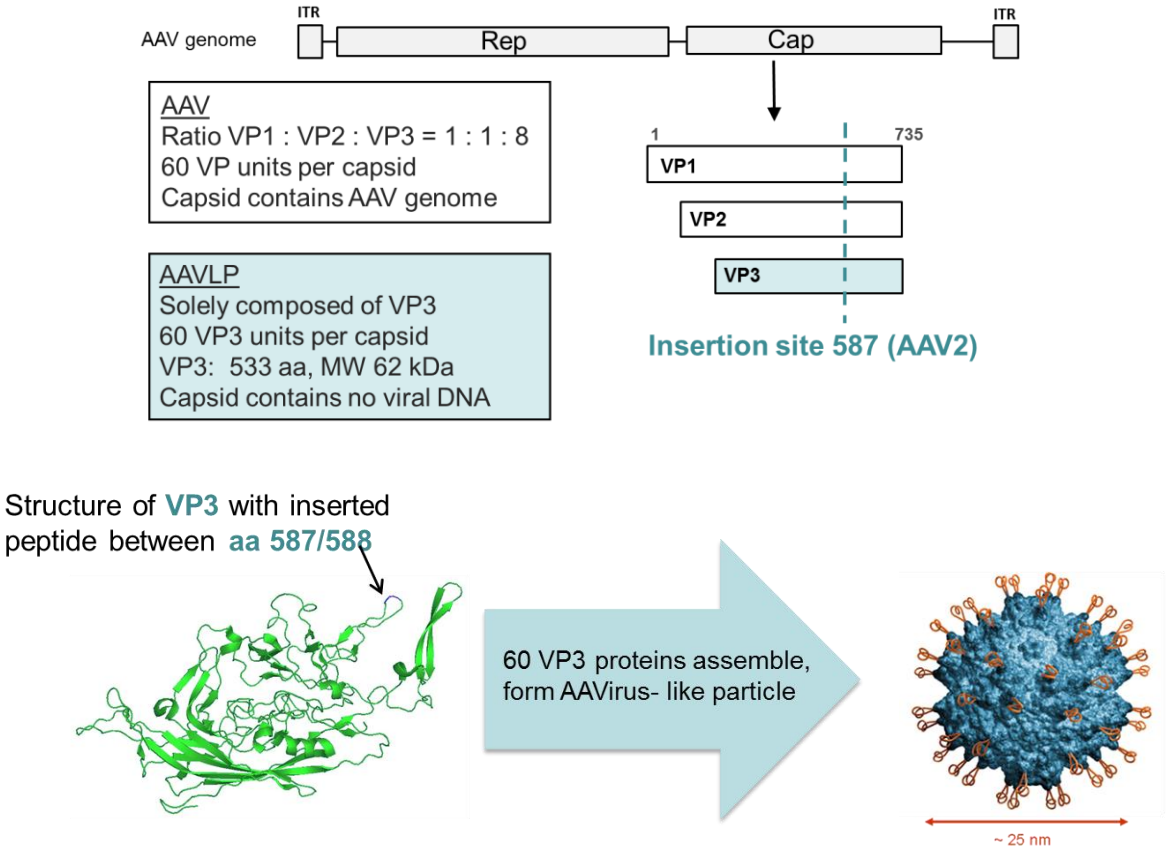

Figure 2.1: Composition of AAVs and AAVLP particles used in this master thesis. AAV capsid protein VP3 is a N-terminally shortened version of VP1 and VP2. Insertion site 587 is located in the C-terminal region.

All particles were adjusted to equal concentrations and tested for specific antigenicity before further experiments.

AAVLP	AAV	
AAVLP – OVA epitope	**AAV – HER-2 mimotope**	
OVA aa 323-339	HER-2 mimotope	
100µg/mL → 1.6E + 13 particles/mL	100µg/mL → 1.6E + 13 particles/mL	
AAVLP – TP18	**VP3 – TTSN**	**wtAAV**
cholesterol ester transfer protein	random control peptide	w/o control peptide
100µg/mL → 1.6E + 12 particles/mL	100µg/mL → 1.6E + 13 particles/mL	

2.1.2 Mice

Eight weeks old female BALB/c mice were purchased from Charles River (Sulzfeld, Germany). All experiments were approved according to the European Community rules of animal care with the permission of the Austrian Ministry of Science (BMWF-66.009/0003-II/3b/2011).

2.1.3 Cells

- D2F2 is a breast cancer cell line derived from BALB/c mice. The term D2F2-E2 describes this cell line being transfected with human HER-2 (kindly provided by Prof. Wei-Zen Wei, California).
- CT26 is a murine colon carcinoma cell line, termed TAUF1.1 in HER-2 transfected state (kindly provided by Prof. Manuel Penichet, UCLA, California).
  D2F2, D2F2-E2, CT26 and TAUF1.1 – cells were cultured in IMDM media supplemented with 10% FCS, 4mM L-glutamine, penicillin (100U/mL), streptomycin (100µg/mL) and 50µg/mL geneticin G418.
- Lec-HER-2 cells, lymphatic endothelial cells from chinese hamster transfected with HER-2 secrete recombinant (r)HER-2 into the supernatant and are a kind gift of Prof. Do Leaky from John Hopkins University. These cells were maintained in DMEM/F-12 media supplemented with 5% FCS, penicillin (100U/mL), streptomycin (100µg/mL) and 50µg/mL geneticin G418.
- BT474 is a human breast cancer cell line overexpressing HER-2. When termed mBT474, the same cell line has been once passaged through *in vivo* culture in a SCID mouse, kindly provided by the group of Prof. Walter Berger, Cancer Research Instiute, Medical University of Vienna. The culture was performed in α-MEM media supplemented with 10% FCS, 4mM L-glutamine, penicillin (100U/mL) and streptomycin (100µg/mL).
- RBL-2H3 basophil cells were provided from Prof. Arnulf Hartl (Paracelsus University of Salzburg, Austria). Cells were cultured in RPMI 1640 media

supplemented with 10% FCS, 4mM L-glutamine, 2mM sodium pyruvate, 10mM HEPES, 100µM 2-mercaptoethanol, penicillin (100U/mL), and streptomycin (100µg/mL).

2.2 Methods: AAVLP OVA experiment

2.2.1 Mouse immunization

BALB/c mice were immunized with AAVLPs, presenting an OVA epitope (AAVLP-OVA), or the control TP18 epitope (derived from rabbit cholesterol ester transfer protein 18) (AAVLP-TP18). For positive control purposes mice were also immunized with the model allergen OVA (not coupled to AAVLP). By using either aluminum hydroxide (Alum) or Montanide ISA 51 VG® (Mont) as adjuvants, any effects on T_H bias were tested. Altogether a volume of 200µL was given to each individual subcutaneously (s.c.). The detailed immunized protocol is shown in figure 2.2 and table 2.1. Mice were immunized three times with intervals of two weeks, on day 1, 14 and 28. Blood samples were taken before starting the experiment (PIS – pre immune sera) and after each immunization (MIS – mouse immune sera) on days 13, 27 and 41 for testing the immune response against the vaccine.

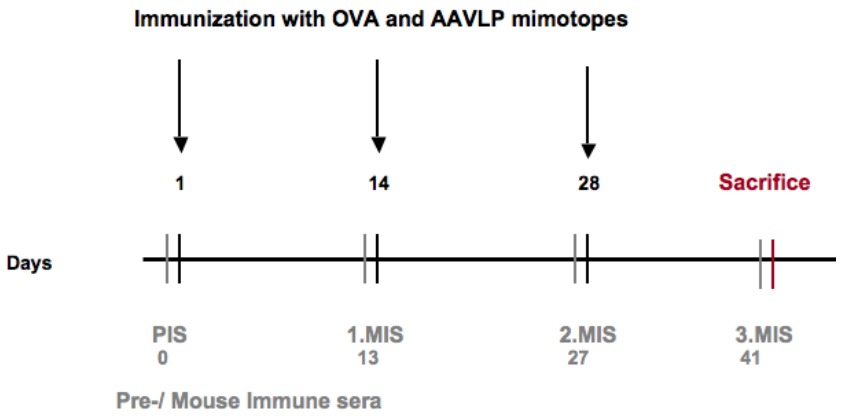

Figure 2.2: AAVLP OVA immunization experiment.

Groups	Adjuvant		Mice/group
A: Naïve			(n=4)
B: OVA (7.2µg in 100µL PBS)	+ Alum (50µL)	+ PBS (50µL)	(n=5)
C: AAVLP-TP18 (100µL)	+ Alum (50µL)	+ PBS (50µL)	(n=5)
D: AAVLP-TP18 (100µL)	+ Mont (100µL)		(n=5)
E: AAVLP-OVA (100µL)	+ Alum (50µL)	+ PBS (50µL)	(n=5)
F: AAVLP-OVA (100µL)	+ Mont (100µL)		(n=5)

Table 2.1: Immunization scheme.

2.2.1.1 *Enzyme-linked immunosorbent assay*

To evaluate specific IgG1 and IgE responses in different immunization groups, blood samples were drawn by tail bleeding after each immunization round and centrifuged following clotting for collecting the sera. Sera were analyzed individually by enzyme linked immunosorbent assay (ELISA). OVA (c=2µg/mL) or wtAAVLP (c=5.0E + 9 capsids/well) were coated overnight at 4°C, 100µL/well. Wells were washed five times (200µL/well) with 0.05% Tween 20 in Tris buffered saline (TBST). After blocking with 1% milk powder/TBST, mouse sera were diluted 1:10 for IgE and 1:100 for IgG1 in 0.1% milk powder/TBST and incubated over night at 4°C. Standard IgG1 and standard IgE were solubilized in 0.1% milk powder/TBST and incubated with a starting concentration of 500ng/mL, in 1:2 serial dilutions. Wells were washed before the incubation with primary detection antibodies rat-anti-mouse IgG1 and rat-anti-mouse IgE. After washing the secondary detection antibody, goat-anti-rat-IgG-HRP, each 100µL/well was incubated for one hour at room temperature and one hour at 4°C. The reaction was developed with ABTS solution (citric acid buffer, 1mg/mL ABTS, 0.1% H_2O_2) and the color reaction evaluated at an optical density of 405nm – 490nm with a microplate reader.

2.2.1.2 *β-hexosaminidase-release assay*

To evaluate the anaphylactogenic potential of the AAVLP vaccine, mouse sera were tested in a β-hexosaminidase-release assay. β-hexosaminidase is released during degranulation of mast cells. RBL-2H3 basophil cells were plated with a concentration of $4x10^4$ in 100µL/well in a 96-well round bottom plate to adhere overnight at 37°C at 5% CO_2. Cells were passively sensitized with pooled mouse sera diluted 1:10 for two hours at 37°C at 5% CO_2. Supernatants were then discarded and cells were washed twice with 0.1% BSA/Tyrode's buffer (200µL).

1L Tyrode's buffer: 9.5g tyrode salts, 0.2g $CaCl_2$, 0.2gKCl, 0.0469g $MgCl_2$(anhyd.), 8g NaCl, 0.05g $NaH_2PO_4.H_2O$, 1g D-Gucose, 2.38g 10mM HEPES, 1g $NaHCO_3$, ad 1L H2O, pH=7.2

For the stimulation ovalbumin, Phl p 5 as irrelevant allergen (0.1µg/mL, 0.5µg/mL, 1.0µg/mL in 100µL/well) and ionomycin as positive control (0.4µg in 100µL/well) were diluted in Tyrode's buffer without any allergen and 10% Triton X-100 were supplemented (10µL) for 10 minutes to achieve 100% β-hexosaminidase-release. 50µL of supernatant were transferred to a flat bottom plate and incubated with 50µL of β-hexosaminidase assay solution [5mL citrate buffer (0.1M citric acid, pH=4.5), 80µL 4-MUG] for one hour at 37°C. Reaction was stopped by adding 100µL glycine buffer (15g glycine, 11.7g NaCl, 1L H_2O, pH=10.7) and fluorescence was measured

at 360-465nm in a fluorometer (Cytofluor 2350, Millipore). Results were calculated as % of the total release.

2.2.2 **Anaphylaxis experiment**

To study safety aspects *in vivo,* allergy and anaphylaxis experiments were performed after the three immunizations. To induce anaphylactic reactions, mice were challenged intravenously with OVA (1mg/ml in 50µL 0.9% NaCl). Rectal temperature was measured before and 20 minutes after the challenge.

2.2.2.1 ***Type I skin test***

For *in vivo* type I hypersensitivity skin testing, naïve and OVA sensitized mice (n=5 per group) were used. OVA, in combination with aluminum hydroxide, a known T_H2 adjuvant, was vaccinated three times intraperitoneally to achieve hypersensitivity.
100µL Evans blue (c = 5mg/mL) were injected into the tail vein of mice. Subsequently, 30 µL of 48/80 histamine releasing substance (40µg/mL) as positive control, 30 µL of OVA (5µg/mL) and AAVLP-OVA particles (1.2E + 13 capsid/mL) were administered intradermally into the shaved abdominal skin. For negative control purposes 30 µL of irrelevant allergen Phl p 5 (5µg/mL), wtAAVLP (1.0E + 13 capsid/mL) and PBS were used. After 20 min mice were euthanized and type I responses evaluated. Upon specific mediator release the abdominal skin is colored blue due to vascular leakage.

2.2.2.2 ***Spleen cell preparation***

Spleens of sacrificed mice were removed to isolate immune cells. Spleens were prepared in Petri dishes with RPMI 1640 media supplemented with 10% FCS, 2 mM L-glutamine, penicillin (100 U/mL), and streptomycin (100µg/mL). To receive a cell suspension, spleens were meshed and filtered through 70µm nylon sieve, which were layered over 5mL Lympholyte. Lymphocytes were extracted by density separation via centrifugation at 2240rpm for 20 minutes and washed three times with 10mL media by centrifugation at 1500rpm for 10 minutes. Cells were cultivated in a concentration of $4x10^5$/well in sterile 96-well round-bottom plates and stimulated with 20µg/mL OVA, 20µg/mL Phl p 5, for positive control purposes with 5µg/mL Concavalin A and for negative control with media for 72h at 37°C. After incubation, plates were centrifuged 5 minutes at 1500rpm. 170µL of the supernatant were removed and transferred into a 12 well flat-bottom plate were it was stored at -20°C until further use for cytokine testing.

2.2.2.3 *IL-5 Cytokine ELISA*

Supernatants of stimulated spleenocytes were analyzed for IL-5 production using the IL-5 ELISA-Kit from eBioscience according to the manufacturer's instructions.

2.3 Methods: AAV HER-2 mimotope experiment

2.3.1 **Cell culture**

Cells [D2F2-E2, D2F2, TAUF1.1, CT26, (m)BT474] were suspended in 10mL media and centrifuged at 1200rpm for three minutes. The pellet was resuspended in media (15mL) before cells were seeded in 75cm² cell culture flasks and incubated at 37°C in humidified atmosphere of 5% CO_2. When reaching a confluence cells were split to maintain exponential growth. For this purpose cells were washed with 5mL PBS before being trypsinized with 0.05% trypsin – EDTA (1 – 2mL). The enzymatic reaction was stopped by adding an excess of fetal calf serum (FCS), a component of the media. Cell – trypsin – medium suspension was centrifuged at 1200rpm for four minutes, the pellet was resuspended and seeded again in a new flask for incubation at 37°C in a 5% CO_2 atmosphere.

2.3.2 **rHER-2 purification**

Lec-HER-2 cells were cultivated in DMEM/F12 Media supplemented with FCS, L-glutamine, penicillin, streptomycin and geneticin G418, as described above. Cells secrete recombinant HER-2 (rHER-2) into supernatant, which was collected and stored at -20°C until further purification.

2.3.2.1 *rHER-2 purification with Ni-NTA mini columns*

Lec-HER-2 supernatants were mixed with equilibration buffer (NPI-10* buffer, according to manufacturer's instructions, Quiagen Kit) in an 1:5 equation. Ni-NTA mini columns were equilibrated with 600µL NPI-10* by a two minute centrifugation at 2900rpm. Columns were then loaded twice with 600µL supernatant-buffer mixture which was centrifuged at 1600rpm for five minutes. Flow through was removed and columns were then washed twice with 600µL NPI-10* for two minutes at 2900rpm. To eluate the proteins, columns were loaded three times with 300µL NPI-250 and centrifuged at 2900rpm for two minutes.

These eluates were concentrated by centrifugation (3500rpm, 5-8 minutes) with an Amicon ultra-15 centrifugal filter tube and dialyzed over night at 4°C against sterile

aqua double distilled or sterile PBS with a dialysis cassette 10.000 MWCO. Dialyzed rHER-2 was stored at -20°C until further detection.

2.3.2.2 *rHER-2 purification with Ni-NTA agarose beads*

To increase the protein amounts purified from Lec-HER-2 supernatants, we improved the method using Ni-NTA agarose beads instead of mini columns.
NPI-10* buffer was mixed 1:10 with Lec-HER-2 supernatant before Ni-NTA agarose beads (1:100) were added and incubated overnight at 4°C under continuous agitation. The next day supernatant beads mixture was loaded onto a polyprep column which was washed with 15mL NPI-10* buffer. Eluation was done step by step with 100µL to 150µL with NPI-250 buffer.
Eluates were concentrated, dialyzed and stored as mentioned before.

2.3.2.3 *SDS polyacrylamide gel electrophoresis*

Sodium dodecyl sulfate polyacrylamide gel electrophoresis (SDS PAGE) is a method that separates a protein according to its mass. Electrophoretic mobility independent on molecular charges in the gel is guaranteed by charging the protein negatively with SDS (provided by Laemmli sample buffer). For HER-2 detection an 8% polyacrylamide gel was prepared:

Separation	gel		Stacking	gel	
	Aqua dest.	4.76mL		Aqua dest.	2.4mL
	Running buffer	2.5mL		Stacking buffer	1.25mL
	10% SDS	100µL		10% SDS	50µL
	30% Acrylamide	2.6mL		30% Acrylamid	1.3mL
	10% APS	50µL		10% APS	25µL
	TEMED	10µL		TEMED	10µL

Table 2.2: 8% SDS PAGE.

Purified proteins were mixed at equal parts with reducing loading buffer and were incubated for three minutes at 95°C. Prepared samples and the marker PageRuler^{TM} Plus prestained protein ladder (Thermo Scientific) were loaded onto the PA Gel and run at 200V, 60mA in electrophoresis buffer for one hour. Afterwards the gel was rinsed in water before it was stained for two hours with Coomassie brilliant blue and destained over night with Coomassie destainer.

2.3.2.4 *Protein detection with Pierce BCA protein assay*

For quantification of purified HER-2, Piece BCA protein assay kit was used as detection method according to the manufacturer's instructions. A standard curve with different concentrations of BSA was plotted, setting up an appropriate equation for calculating the concentration of purified HER-2.

2.3.3 Flow cytometric analysis

For chosing a tumor cell line for the tumor transplantation experiment, flow cytometric analysis was performed to verify HER-2 surface expression. The HER-2 expressing D2F2-E2 and TAUF1.1 tumor cells were compared to the non-HER-2 expressing D2F2 and CT26 tumor cells. Therefore, cells were harvested, counted and portioned in a concentration of 2.5 x 10^5 cells in 1mL FACS buffer (PBS, 5% normal goat sera) per tube. Tastuzumab and controls were added into appropriate samples, mixed and incubated at 4°C for 30 minutes. Cells were washed with 2mL FACS buffer by centrifugation at 1200rpm for three minutes, before adding the secondary FITC labeled antibody to resuspended cells. After an incubation at 4°C for 30 minutes, cells were washed again with 2mL FACS buffer and afterwards solubilized in 500µL FACS FIX buffer (FACS buffer, 1% paraformaldehyd) for analysis using FACS Calibur.

2.3.4 Tumor titration experiments

For tumor transplantation, a defined tumor cell line had to be chosen, comparing D2F2-E2 and TAUF1.1 with the non-HER-2 expressing cell lines D2F2 with CT26, respectively. For this purpose, an *in vivo* titration experiment was performed using naïve female BALB/c mice.

After reaching appropriate cell density, cells were resuspended in PBS and adjusted to cell numbers of 1x10^6 or 1x10^7 in 100µL solution, and injected subcutaneously into naïve BALB/c mice. D2F2-E2 cells were implanted on the right flank, D2F2 on the left side using the same cell number. In the other groups of mice, CT26 cells were implanted on the right flank and TAUF1.1 on the left side, again using the same cell number in each individual. 1x10^6 tumor cells were transplanted into two mice each and 1x10^7 into four mice. Tumor growth was monitored by palpation and caliper measurement every day.

2.3.5 **Specificity test of HER-2 mimotopes displayed by AAV particles**

All AAV HER-2 mimotope clones and the carrier wtAAV were tested for specificity in ELISA. 100µL/well of 1µg/mL anti-HER-2 antibody trastuzumab (Herceptin®) and as isotype controls the anti-CD20 antibody rituximab, as well as the anti-EGFR antibody cetuximab were coated onto ELISA plates and incubated overnight at 4°C. After blocking with 1% BSA in PBST (0.05% Tween) for one hour at room temperature and one hour at 4°C, followed by washing with PBST, particles were diluted in 0.1% BSA / PBST in the following concentrations:

DMD1, DMD2, wtAAV (negative control): 1µg/mL, 0.5µg/mL, and 0.1µg/mL, (here, clones DMD1 and DMD2 are exemplarily applied).

The particles were incubated under soft agitation for 2 hours at room temperature before they were washed again. Anti-AAV antibody was diluted 1:20 in 0.1%BSA / PBST and incubated for one hour at 37°C. For detection streptavidin-HRP was diluted 1:1000 in PBST and incubated for another hour at room temperature. The reaction was developed with ABTS substrate solution and the color reaction recorded at an optical density of 405nm – 490nm in a microplate reader.

2.3.6 **Mouse immunization I.**

AAV particles displaying different HER-2-mimotopes on their surface (table 2.3) were used for immunizations of eight weeks old female BALB/c mice (n=8). Vaccination was performed subcutaneously into the nuchal fold three times with intervals of two weeks (figure 2.3). In this first approach Montanide ISA 51 VG® was used as adjuvant.

Groups/ Particles		Concentration	Montanide®
A/ DMD1	100µL	100µg/mL	100µL
B/ DMD2	100µL	100µg/mL	100µL
C/ DMD4	100µL	100µg/mL	100µL
D/ DMD15	100µL	100µg/mL	100µL
E/ DDD19	100µL	100µg/mL	100µL
F/ VP3-TTSN(*)	100µL	100µg/mL	100µL
G/ Naïve			

Table 2.3: Immunization groups of HER-2 experiment I.

To evaluate specific immune responses in different immunization groups, blood samples were drawn by tail vein bleeding after each vaccination round to gain mouse sera.

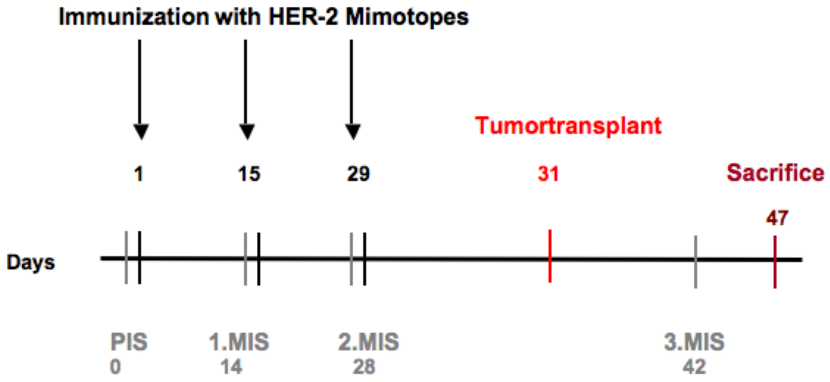

Figure 2.3: AAV HER-2 mimotope immunization experiment I.

2.3.7 **ELISA for testing immunogenicity against rHER-2**

According to the protocoll described above in 2.3.1.1, pre-/ mouse immunsera were analyzed individually by ELISA for immunoglobulin reactivity against rHER-2 (coating 1µg/mL). After blocking and washing, mouse sera were diluted 1:100 for total IgG. As positive control trastuzumab and as negative control rituximab were used. Wells were washed before incubation with detection antibody anti-mouse-IgG-HRP (for sera detection), or anti-human-IgG-HRP (for control detection), each 100µL/well, for one hour at room temperature and one hour at 4°C. The reaction was developed with ABTS solution and color reaction evaluated at an optical density of 405nm – 490nm.

2.3.8 **Immunofluorescence**

D2F2 and D2F2-E2 were seeded for a concentration of $2x10^5$ cells in 400µL per well on four-well immunofluorescence chamber slides (Permanox®, Thermo Scientific). After 24 hours they were fixed with 4% paraformaldehyde for 8 minutes at room temperature before they were washed three times with cold PBS. For DAPI staining, cells were permeabilized 5 minutes with 0.5% TritonX-100 in PBS and washed again with cold PBS. Sera were diluted 1:20 in PBS/ 0.5% BSA with 200µL each well, whereas trastuzumab and rituximab were incubated with 1µg/mL each. After an incubation of one hour at room temperature, wells were washed four times with cold PBS, before the secondary antibody, diluted 1:200 in PBS/ 0.5% BSA was added in 400µL per well. Incubation was performed by covering slides with aluminum foil for 45

minutes, and stopped by washing slides four times with cold PBS. DAPI diluted 1:5000 was incubated for eight minutes at room temperature and then washed three times with cold PBS.

Afterwards all slides were washed in distilled aqua before they were covered with mounting medium (Fluoromount^{TM}, Sigma) and stored at 4°C.

2.3.9 **Tumor transplantation I.**

After deciding on the tumor cell clone D2F2-E2 and D2F2 with cell numbers of $1x10^7$ per mouse, cells were cultured for the transplantation experiment. Cells were washed with PBS and trypsinized before they were counted and diluted in sterile PBS. D2F2 cells were implanted on the left flank, D2F2-E2 on the right side using same cell numbers ($1x10^7$ in 100µL). Remnants were used for FACS analysis to verify correct HER-2 expression directly before grafting. Tumor growth was monitored by caliper measurement at a daily basis to plot a growth curve.

2.3.10 **Mouse immunization II.**

Medigene supported new HER-2 AAV mimotope clones, which were this time immunized (n=8 per mouse group) with aluminum hydroxide instead of Montanide ISA as an adjuvant (table 2.4). To achieve a better immune response, four immunizations were planned with intervals of ten days (figure 2.4).

Groups/ Particles		Concentration	Alum
A/ DMD1	100µL	100µg/mL	100µL
B/ DMD2	100µL	100µg/mL	100µL
C/ DMD4	100µL	100µg/mL	100µL
D/ DMD6	100µL	100µg/mL	100µL
E/ DMD15	143µL	70µg/mL	100µL
F/ DDD19	120µL	83µg/mL	100µL
G/ DMM44	100µL	100µg/mL	100µL
H/ wtAAV	143µL	70µg/mL	100µL
J/ rHER-2	100µL	50µg/mouse	100µL
K/ Naïve			
L/ 4D5	100µg/mouse	2.5mg/mL	passive Imm.

Table 2.4: Immunization groups of HER-2 experiment II.

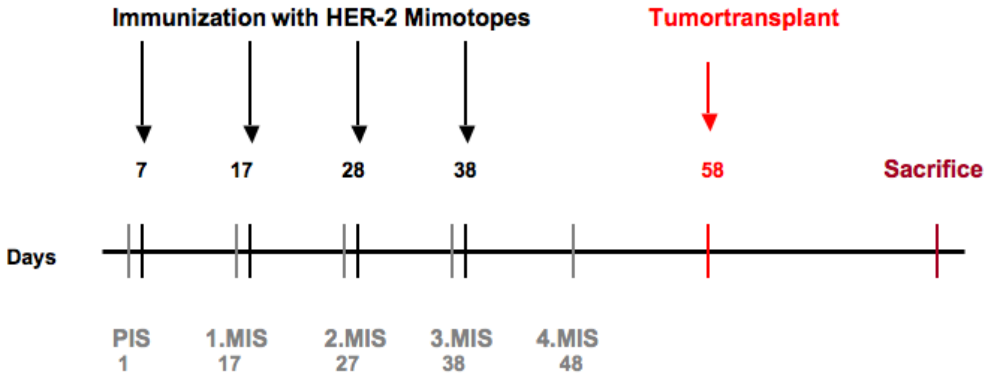

Figure 2.4: AAV HER-2 mimotope immunization experiment II.

2.3.11 **ELISA for testing immunogenicity against rHER-2**

To test the immune response resulting from the second AAV HER-2 mimotope vaccination, ELISA was performed comparing the immunoglobulin reactivity against rHER-2 of pre immune sera and 1st to 4th mouse immune sera according to the protocol described above in 2.3.7, using the antibodies rat anti-mouse IgG1 and goat anti-rat IgG-HRP for detection.

2.3.12 **Tumor transplantation II.**

After complete immunization, a repetition of the *in vivo* tumor experiment was performed. This time, only the HER-2 expressing cell line D2F2-E2, with a cell number of 1x10^7 was chosen.

As an additional control, 4D5 antibody, the murine precursor of the clinically used humanized anti-HER-2 antibody trastuzumab was passively applied (100µg/mouse) as positive control by passive immunization. Also rHER-2 was used as a control immunogen solubilized in sterile PBS (50µg/mouse).

Because of the invasive and aggressive tumor growth of D2F2 cells, only the HER-2 expressing cell line, D2F2-E2 was used for further tumor transplantation, but cell numbers 1x10^7 remained unchanged due to most homogeneous growth behavior.

2.3.13 **Histology**

Tumors of sacrificed mice were collected, washed with PBS and chemically fixed in 4% paraformaldehyde to avoid autolysis, decay and decomposition. Paraffin is insoluble in water and in alcohol, so four steps were necessary for embedding: dehydration, intermediate, saturation in paraffin and solidification. In the last step

tumors were formed into blocks by paraffin effusion and by cooling them down quickly. Afterwards paraffinated tumor blocks of naive, rHER-2 and 4D5 group were cut into 4µm sections and histologically stained with hematoxilin – eosin, which colors nuclei blue and eosinophilic structures in different red colors. For testing HER-2 expression directly on tissue, sections were immunohistochemically stained with HerceptTest®, where membrane bound HER-2 is colored brown and the rest is stained blue (kind support by Prof. R. Horvath, Clinical Institute of Pathology, Medical University of Vienna).

2.3.14 **Proliferation assay**

D2F2-E2, D2F2, TAUF1.1, CT26, BT474 or mBT474 cells were seeded in 96-well round-bottom plates with a concentration of $2x10^4$ cells in 100µL media and incubated over night at 37°C in a humidified atmosphere of 5% CO_2.

After 24 hours, cells were stimulated with 1µg/well trastuzumab, rituximab or cetuximab solubilized in sterile PBS. Alternatively, purified mouse IgGs from AAV-mimotope immunized mice (5µg/well) was applied (protocol for antibody purification listed below). For control purposes 1µg/well of 4D5 was used. For further control purposes cells alone and media alone were also used. After 24, 48, 72 hours 10µl/well EZ4U® assay substrate (tetrazolium-based) was added and incubated for three hours at 37°C. Supernatants were transferred into 96-well flat-bottom plates and the signal determined at optical density of 450nm – 620nm using a microplate reader.

2.3.15 **Antibody purification**

For proliferation assays, HER-2 specific antibodies were purified from preimmune sera and fourth immune sera with protein G sepharose beads. Single sera of groups were pooled at equal parts. 150µL or 250µL protein G sepharose beads with a binding capacity of around 20mg/mL were added into each pool of PIS and 4^{th} MIS. The sera/beads mixture was incubated overnight at 4°C under constant agitation. On the next day, the mixture was spun down and Ni-NTA columns were equilibrated with 1mL 10mM Tris/HCl. Afterwards sera/beads mixtures were loaded and the flow through collected. Columns were washed with 2mL 100mM Tris/HCl and then with 2mL 10mM Tris/HCl buffer before they were eluted twice with 1mL 0.1M glycine at pH 2.5 and neutralized with 1/10 1M Tris/HCl.

Eluates were afterwards loaded onto MicroSpin™ columns to make a buffer exchange from a glycine Tris/HCl buffer to aqua double distilled.

Consequently, quality of purified IgG antibodies was tested by SDS PAGE and specificity by ELISA, coating 1µg/mL rHER-2 and using 1µg/mL 4D5 antibody for control purposes (according to the protocol described in 2.3.7). Purified antibodies were adjusted to 3µg/mL for incubation and tested for the presence of IgG1, IgG2a or IgG2b antibodies. Rat anti-mouse IgG1, IgG2a or IgG2b were used as primary antibodies and goat anti-rat IgG-HRP for detection using TMB substrate for development. Substrate A and B were mixed at equal parts pipetting 100µL into each well. The reaction was stopped with 100µL/well 1.8M H_2SO_4 and detected at an optical density of 450nm – 630nm in a microplate reader.

3 Results

3.1 AAVLP OVA experiment

3.1.1 **Immunogenicity of AAVLPs**

In the first part of this thesis project AAVLPs were examined for immunogenicity and safety using an 18 amino acid OVA B-cell epitope displayed by AAVLPs as a model system. Mice were immunized three times in bi-weekly intervals and the induced IgG1 and IgG2b antibodies were monitored by ELISA, comparing the preimmune antibody titers (PIS) with those induced by 1st – 3rd MIS. The allergen OVA was coated for determining the antigen specific response, wtAAVLP particles were coated for evaluating the anti-carrier response. The columns in figure 3.1 A – D indicate mean values plus/minus standard deviation of all determined single values. As expected, all mice immunized with AAVLP presented comparable anti-carrier responses (figure 3.1 B.). In contrast, only groups immunized with the OVA peptide displayed by AAVLPs developed an OVA-specific IgG1 response (figure 3.1 A.). The induced IgG was dominated by IgG1, whereas antibody class IgG2b was only detectable at background levels (C. and D.). Groups immunized with Alum as adjuvant showed higher specific IgG1 antibody titers, than groups vaccinated with Montanide. Moreover, antibody titers were not only higher, but also more homogeneous in sera vaccinated with aluminum hydroxide than with Montanide. This is illustrated in E. and F., where results of single sera are shown individually.

A

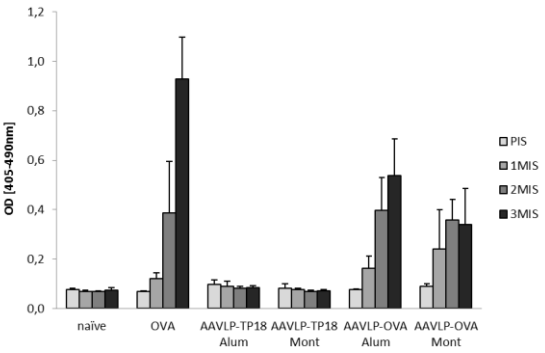

B

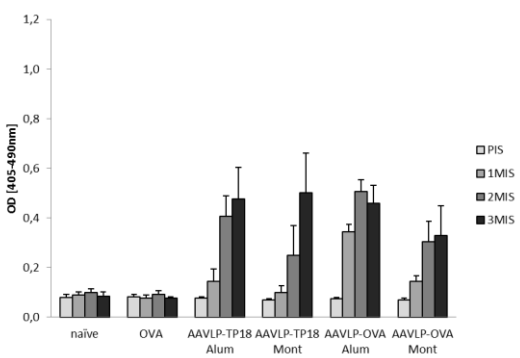

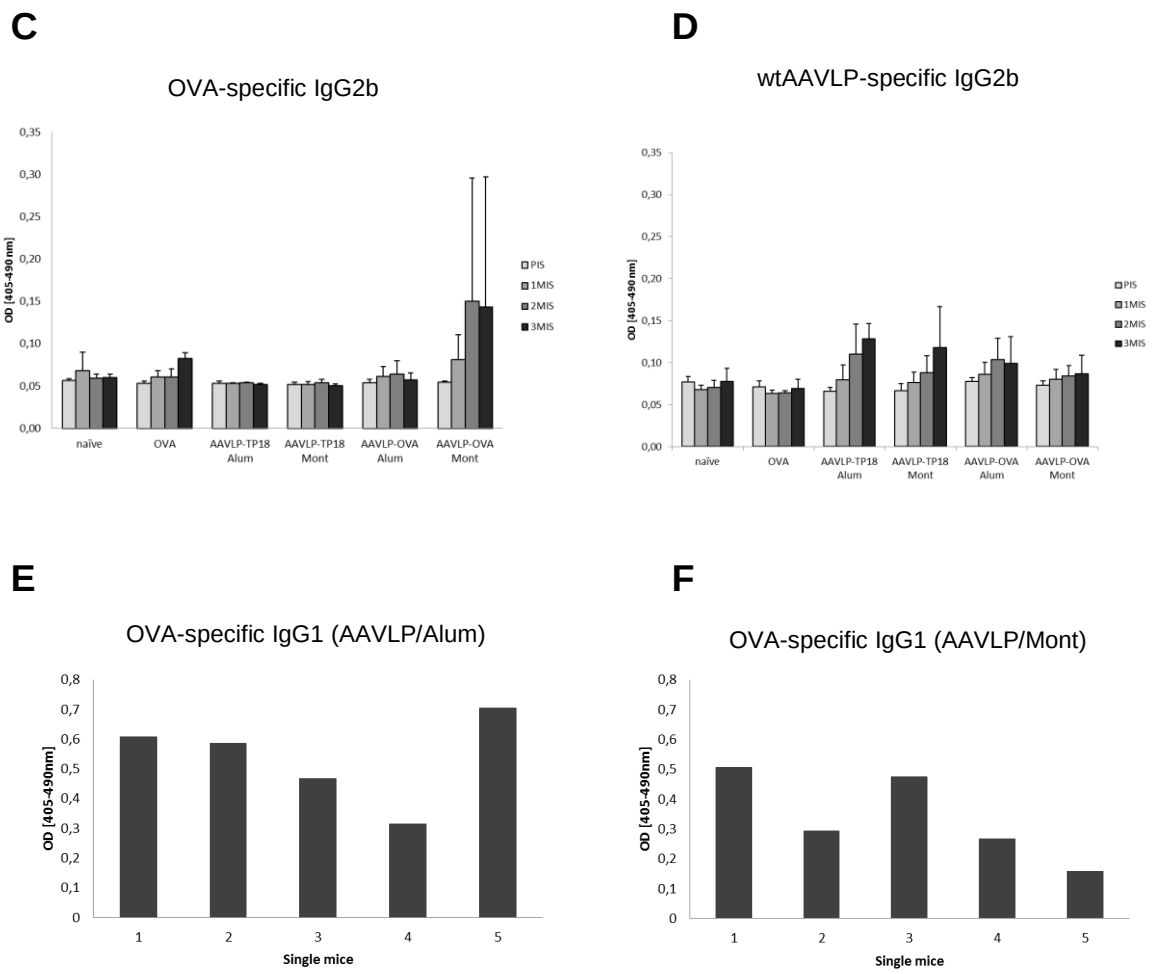

Figure 3.1: Specific antibody detection by ELISA. A.: OVA-specific IgG1. B.: wtAAVLP-specific IgG1. C.: OVA-specific IgG2b. D.: wtAAVLP-specific IgG2b. E.: OVA-specific IgG1 of 3rd MIS AAVLP/Alum. F.: OVA-specific IgG1 of 3rd MIS AAVLP/Mont.

3.1.2 *In vitro* safety aspects of AAVLPs

The question whether AAVLP displayed mimotopes would induce hypersensitivity was addressed by *in vitro* experiments. First, it was tested whether IgE, the anaphylactogenic class of immunoglobulins, was induced by any of the treatments or vehicles. Figure 3.2 A. shows that there was no IgE in any of the AAVLP-immunized groups. To evaluate the functional anaphylactogenic potency of the AAVLP vaccine, mouse sera were pooled of each group and analyzed using a β-hexosaminidase-release assay. RBL (rat basophile leukemia) cells harbor the high affinity IgE receptor and may be sensitized with IgE by serum incubation, in case IgE is contained. Upon allergen challenge, RBL release from their granula β-hexosaminidase. Because of the fact, that no IgE was present in AAVLP immunized groups, RBL cells were not able to degranulate and release β-hexosaminidase. Thereby the safety of the vaccine could

be affirmed *in vitro* (figure 3.2 B.). As expected, the reference group “OVA-immunized mice” contained IgE in their sera which was functional in the RBL assay and led to mediator release.

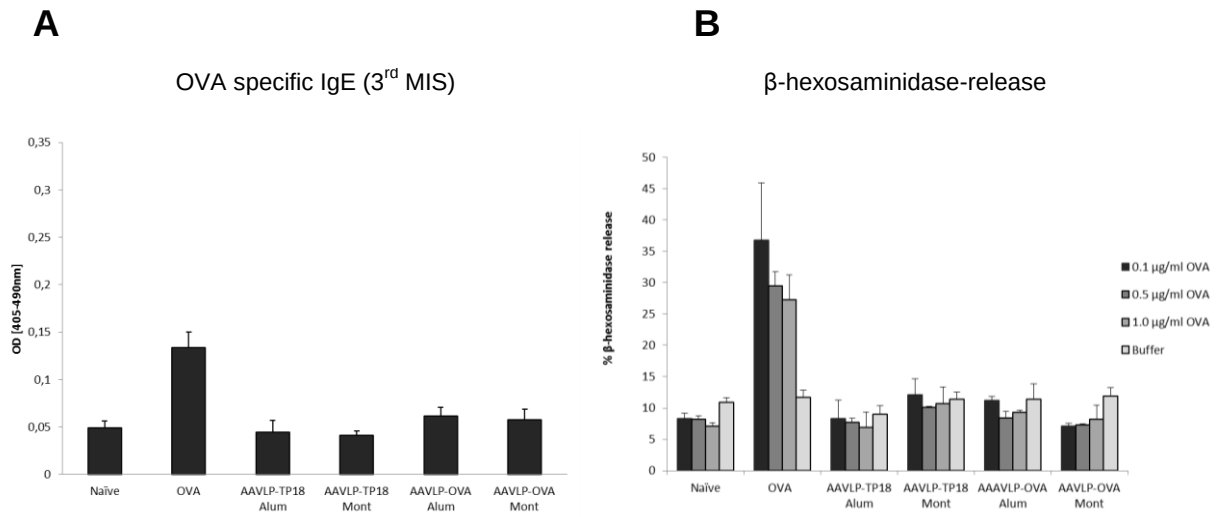

Figure 3.2: A.: IgE (3rd MIS) on OVA in ELISA. B.: β-hexosaminidase-release assay.

Interleukin 5 (IL-5) is a cytokine responsible for eosinophilic granulocyte differentiation. It is secreted by T_H2 helper cells and elevated IL-5 level indicate a T_H2-shift of the immune response. The above observed IgG1 antibodies were suggestive for a T_H2 immunomodulatory property of the AAVLP-OVA vaccine at least in context of the selected adjuvant Alum or Montanide. To further investigate this, spleenocytes were isolated and cultured from the mice of each group, stimulated with OVA and supernatants collected and subjected to cytokine ELISA. Figure 3.3 illustrates AAVLP immunized groups secreting IL-5 only at background levels, whereas higher levels of IL-5, although not significantly, were determined in OVA-immunized group.

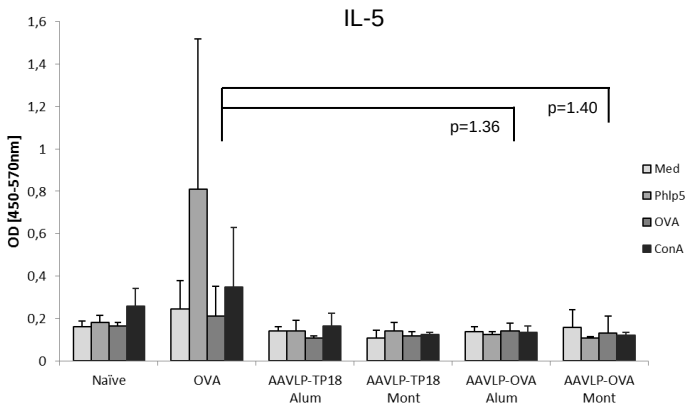

Figure 3.3: Detection of IL-5 cytokine from spleenocytes ELISA. No significance: ns p>0.05.

3.1.3 *In vivo* safety aspects of AAVLPs

3.1.3.1 *Anaphylaxis experiments*

A drop of body temperature is a typical symptom of anaphylaxis and can be easily evaluated. All mice of each group were challenged intravenously with OVA and rectal temperature measured before and 20 minutes after the challenge (figure 3.4). Whereas the OVA-immunized positive control group displayed a significant temperature difference (36.5° - 30.5°C), the AAVLP-OVA immunized groups remained stable, indicating no anaphylactic reaction in any of the AAVLP immunized mice.

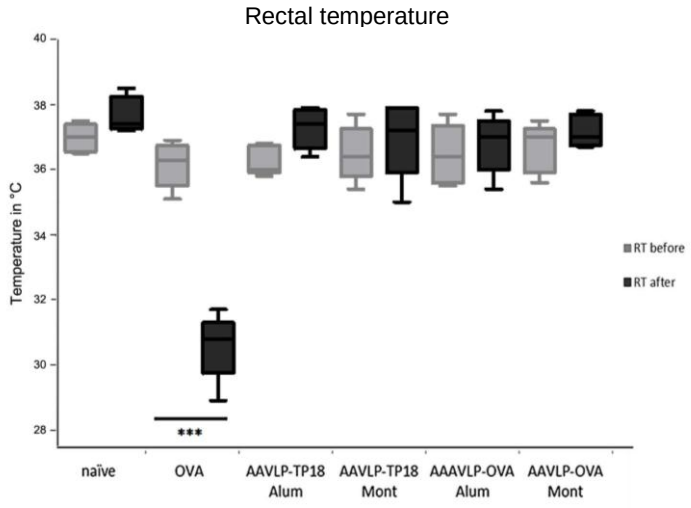

Figure 3.4: Rectal temperature. Significance: *** p<0,001

Physical activity is also reduced during anaphylaxis. Also this typical symptom was exclusively observed in the OVA challenge in OVA-immunized group and mirrored the results of the body temperatures (not shown).

3.1.3.2 *Type I hypersensitivity skin testing*

From the above experiments with the AAVLP-displayed OVA epitope we learned that most likely, the vaccine does not induce allergy, but rather immunity. However, how safe would the vaccine be in an already sensitized organism? This aspect would be relevant for the application of AAVLPs for a possible later development of a vaccine for allergics. Therefore, we additionally tested safety aspects in specifically sensitized mice. Naïve and OVA i.p. sensitized mice were challenged intradermally with substances indicated in figure 3.5. In case an allergen specifically binds to cell-fixed IgE, productive cross-linking and mediator release is achieved, rendering, vascular leakage occurs, visible as blue color exsudating into the skin. In the naïve group only

positive control histamine-releasing substance 48/80 induced a histamine release resulting in blue coloring of the skin. OVA-sensitized mice showed positive reactivity to 48/80 and, as expected, to challenges with OVA. AAVLP-OVA produced negligible coloring. No systemic reactions were observed in any of the challenged mice. This result indicates that in allergic patients, only immediate local side effects may be expected with an AAVLP-vaccine displaying an allergen or allergen subunit. On the other hand no type I skin reactivity was observed from challenges with the carrier AAVLP clones confirming tolerability of the vaccine.

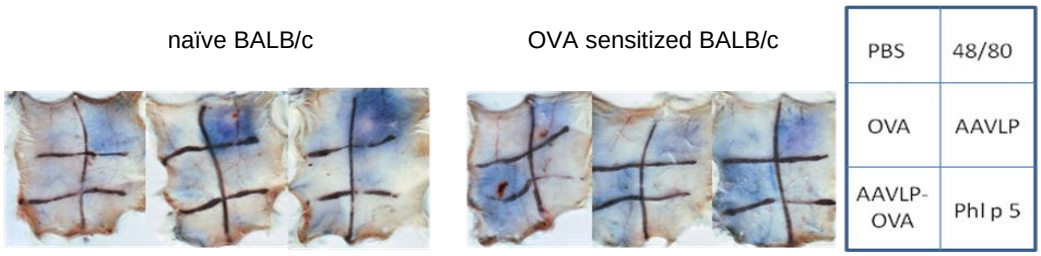

Figure 3.5: Type I skin test of naïve and OVA i.p. sensitized mice. Panels bottom, left; mouse 1: note exsudation of OVA reaction into field.

3.2 AAV HER-2 mimotope experiment

3.2.1 **rHER-2 specificity**

For testing antibody specificity, rHER-2 was produced and quality was proved by a Coomassie blue stained SDS polyacrylamide gel. Figure 3.6 illustrates several protein fragments, due to destruction of hydrogen bonds within the protein induced by β-mercaptoethanol, a component of the sample buffer.

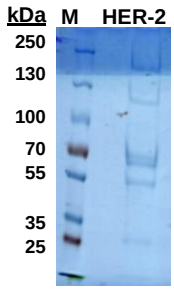

Figure 3.6: Purified recombinant HER-2 analyzed by Coomassie blue stained SDS polyacrylamid gel electrophoresis.

Specificity of purified rHER-2 was affirmed by the anti-HER-2 antibody trastuzumab in ELISA. Negative controls anti-CD20 antibody rituximab and anti-EGRF antibody cetuximab did not bind to rHER-2 and attested therefore specificity of the purified antigen (data not shown).

3.2.2 **Tumor titration experiments**

Before tumor transplantation, flow cytometric analysis was performed to verify HER-2 surface expression of the tumor cells D2F2-E2 and TAUF1.1 compared to non-expressing D2F2 and CT26 tumor cells (figure 3.7). The typical red shift demonstrates HER-2 expression recognized by the monoclonal antibody trastuzumab. Blue indicates isotype control.

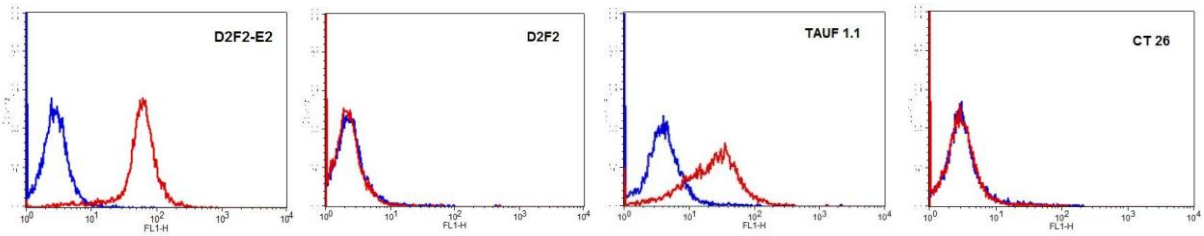

Figure 3.7: HER-2 expression status of D2F2-E2, D2F2, TAUF1.1 and CT26 cells. The characteristic red shift determines HER-2 expression. Blue shows isotype control.

The HER-2 expressing cell lines D2F2-E2 and TAUF1.1 versus the non-expressing D2F2 and CT26 were cultivated and transplanted into naïve BALB/c mice at different cell numbers ($1x10^6$ and $1x10^7$). The growth of HER-2 expressing and non-expressing cells within the same individual was compared injecting each cell type into left or right flank. D2F2 and D2F2-E2 showed a more homogeneous tumor growth than CT26 and TAUF1.1 (figure 3.8). Apparently D2F2 were the most succesfully and homogenously growing transplanted cells of all. With respect to the HER-2 expressing cells D2F2-E2 tumors occurred earlier, abaut day 4, than TAUF1.1, which started growing at day 9. Based on these preexperiments D2F2-E2 and its parental cell line D2F2 were chosen for the following tumor transplant experiments in HER-2 mimotope immunized mice.

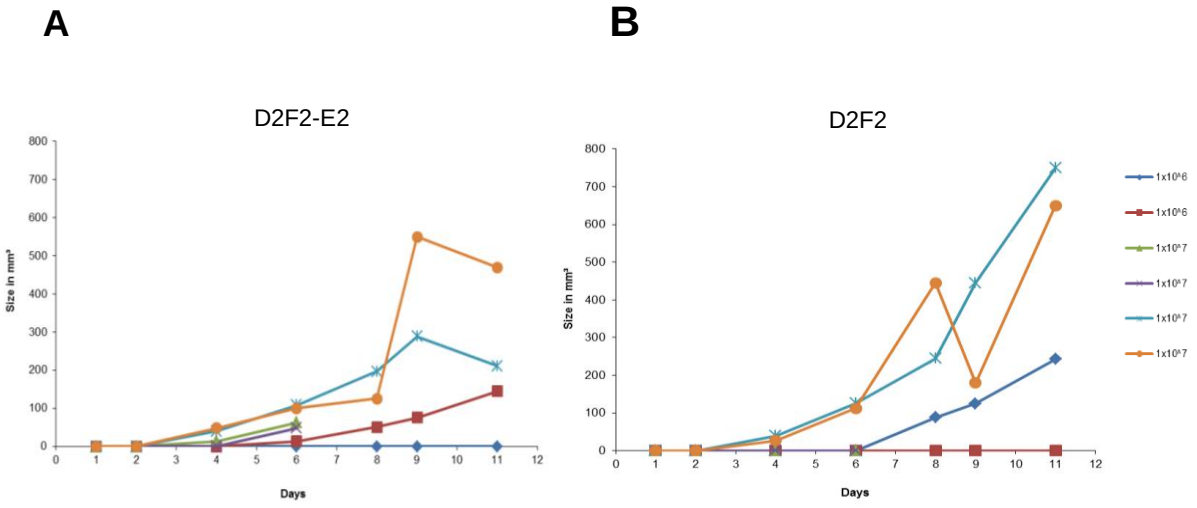

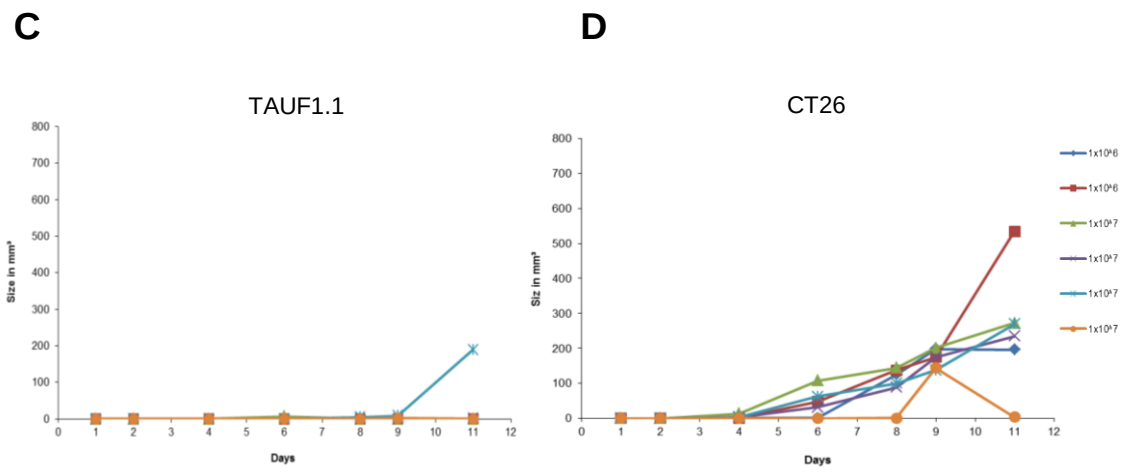

Figure 3.8: Tumor growth cuves of A. D2F2-E2, B. D2F2, C. TAUF1.1 and D. CT26 cells.

3.2.3 **HER-2 immunization experiment I**

3.2.3.1 ***Specificity test of HER-2 mimotopes***

HER-2 mimotopes were selected by Medigene from an AAV display library by the anti-HER-2 antibody trastuzumab. Figure 3.9 illustrates that clones specifically bound to trastuzumab, taking DMD1 and DMD2 as examples (A), whereas the signal against rituximab (B) and cetuximab (C) as negative controls remained negative. Further, empty wtAAV did not give any signal indicating the antigen specificity of the assay. Based on these results the HER-2 mimotope displaying AAV particles were ready for immunization experiments.

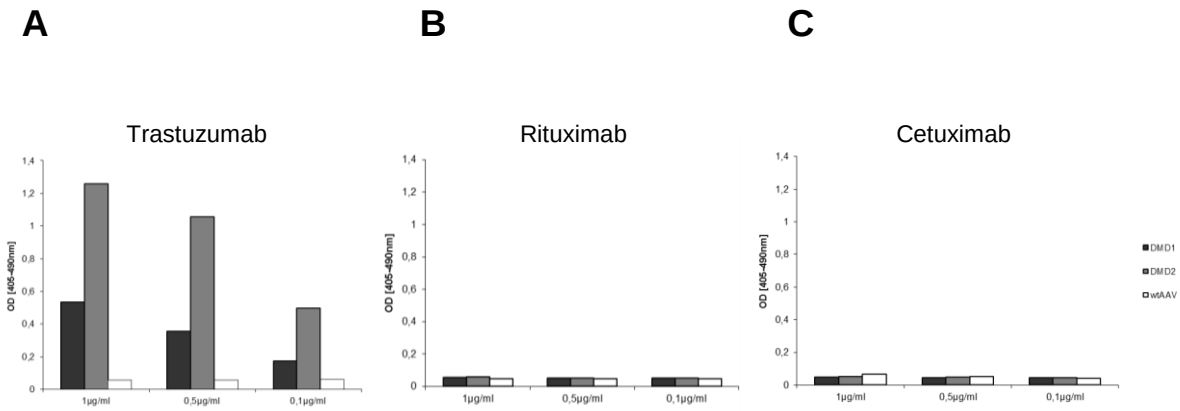

Figure 3.9: The HER-2 mimotope displaying DMD1 and DMD2 particles showed specific binding to the anti-HER-2 antibody trastuzumab in ELISA.

3.2.3.2 *AAV mimotope immunizations prime specific anti-HER-2 IgG*

During the cause of immunization with HER-2 mimotopes, immune sera were collected and tested for the presence of HER-2 specific immunoglobulins in ELISA. Figure 3.10 shows that the IgG response increased during vaccination, also to a certain degree in mice immunized with particles presenting an unspecific peptide TTSN. However, when consecutively all mice were challenged with HER-2 overexpressing D2F2-E2 cells only HER-2 mimotope immunized mice responded with high levels of HER-2 specific total IgG. This result indicates that the AAV mimotope immunizations primed a HER-2 specific immune response against the cellularly expressed antigen. Clone DMD1, DMD2 or DMD15 achieved higher titers against rHER-2 compared to other groups. Homogeneity of the immune response within in one group can be seen in figure 3.11, where individual sera are shown.

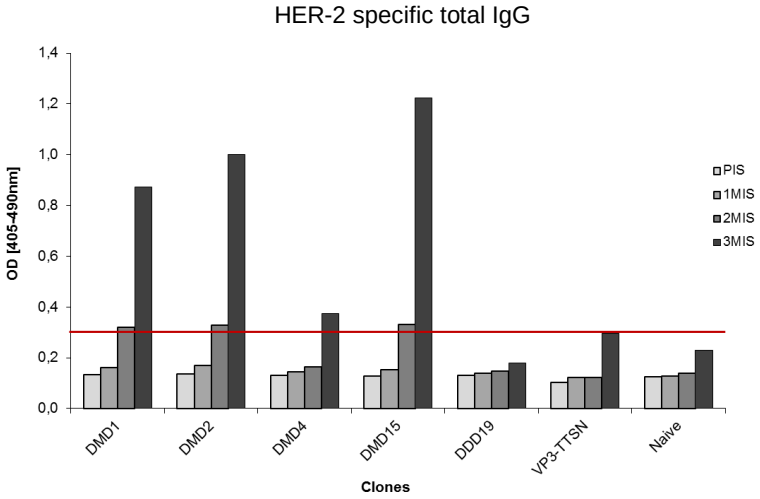

Figure 3.10: Immune response, total IgG of pooled sera on rHER-2.

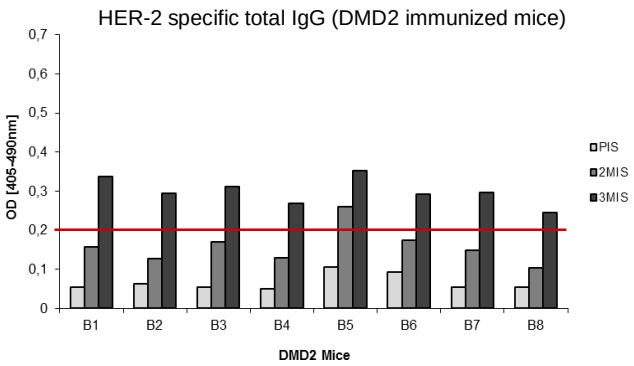

Figure 3.11: The homogeneity of immune response, in mouse groups is demonstrated exemplarily in the group B immunized with clone DMD2. B1-B8 indicate individual mice.

In this immunization experiment Montanide was used as adjuvant, which turned out to be complexe to handle and causing massive granuloma formation.

3.2.3.3 *Immunofluorescence*

To further demonstrate the specificity of the above described immune response, immunofluorescence was performed with the HER-2 overexpressing cell line D2F2-E2 and also for control purposes with the parental cell line D2F2. Exemplarily for all results, immunofluorescence with sera of mice immunized with clone DMD15 is shown in figure 3.12.

DAPI staining of nuclei is visible in blue. HER-2 specific signals are stained by green fluorescence (FITC), the positive control Herceptin demonstrates HER-2 receptor distribution along the membrane. No reaction could be detected in D2F2 cells or in any pre-immune sera. In accordance with ELISA results, a specific signal could only be detected after priming with the natural antigen.

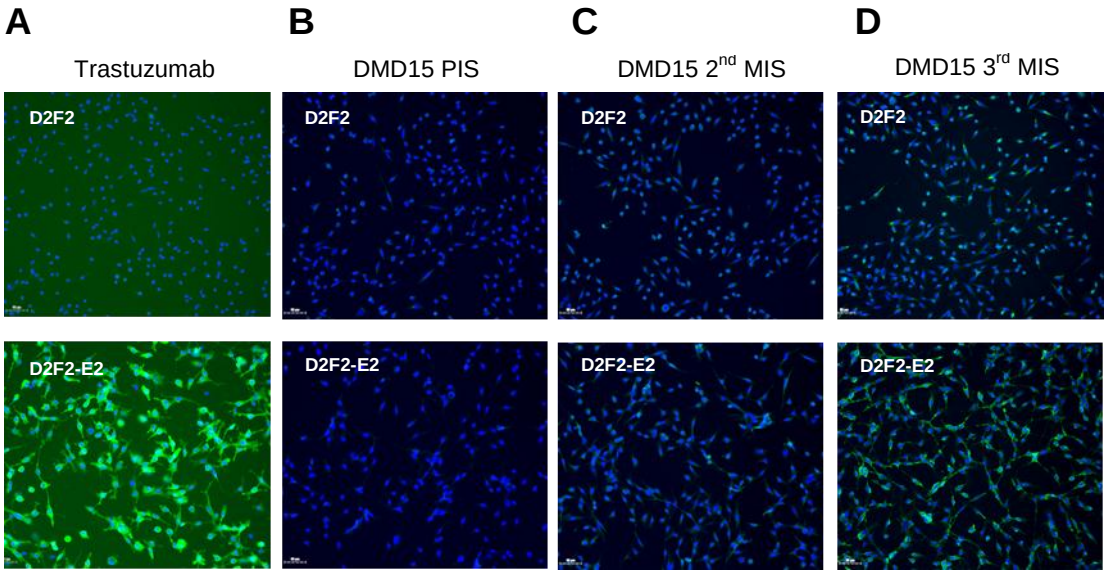

Figure 3.12: Immunofluorescence performed with D2F2 cells and D2F2-E2 cells incubating them with trastuzumab, DMD15 PIS, 2nd MIS and 3rd MIS (from A to D)

3.2.3.4 *Transplantation experiment in HER-2 mimotope immunized mice*

D2F2 cells were implanted on the left flank, D2F2-E2 on the right side of each mouse, using $1x10^7$ cells. Tumors were monitored daily by palpation and caliper measurement (figure 3.13). Albeit the high and specific IgG titers no difference in tumor growth of HER-2 expressing and non-expressing cells could be observed.

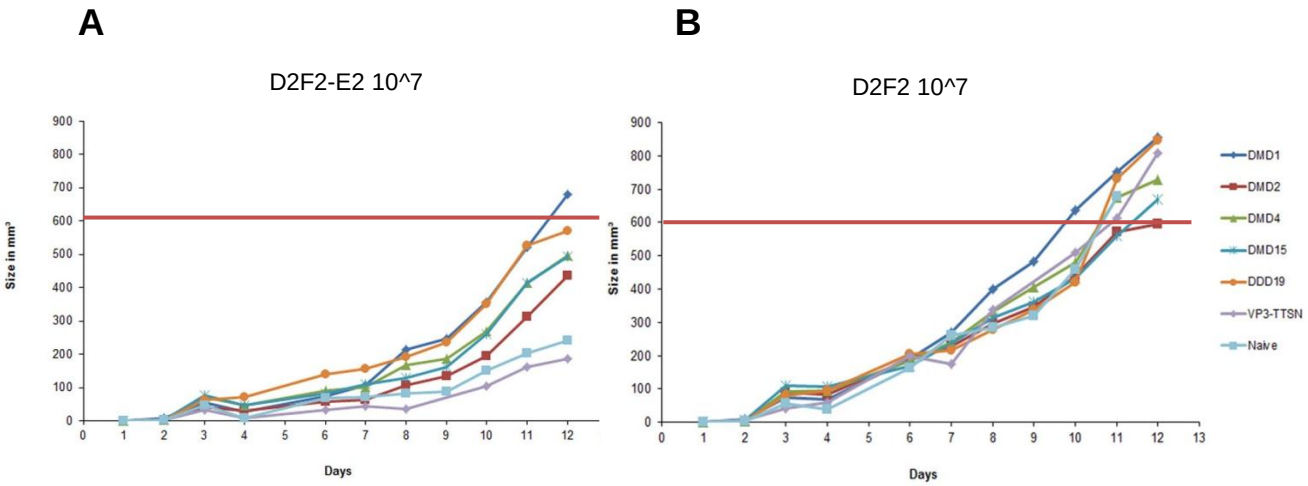

Figure 3.13: D2F2-E2 and D2F2 tumor growth.

Notably, a previously performed tumor transplant experiment in mice immunized with a nonrelated mimotope had shown an effect on tumor growth after 12 days only (Weichselbaumer M. et al. is in progress). The aggressive growth of D2F2 cells in the present experiment did, however not allow maintaining mice alive longer than 12 days. Therefore, an improved experimental design had to be developed for the proof of concept studies, termed HER-2 immunization experiment II, see below.

3.2.4 **HER-2 immunization experiment II**

3.2.4.1 ***AAV mimotope immunizations prime specific anti-HER-2 IgG***

For the repetition and improvement of the mimotope immunization study, clones DMD1, DMD2, DMD4, DMD15, DDD19 were selected again, and DMD6 and DMM44 newly added. For comparison, purified rHER-2 and empty particles were vaccinated in control groups. Further, Alum was used as the adjuvant due to several disadvantages of Montanide (handling, granuloma formation) and the very positive results of the OVA study with Alum. Furthermore, four instead of three immunizations were performed. Again, blood samples of immunized mice were taken and ELISA was performed to evaluate the immune response against HER-2. Figure 3.14 (A.), illustrates that the HER-2 specific IgG1 immune response continually increased during vaccinations in all immune sera. Some AAV mimotopes provoked stronger IgG1 responses than others, whereas homogeneity inside the groups remained stable. Needless to say that the highest IgG1 titers were achieved with purified rHER-2.

A

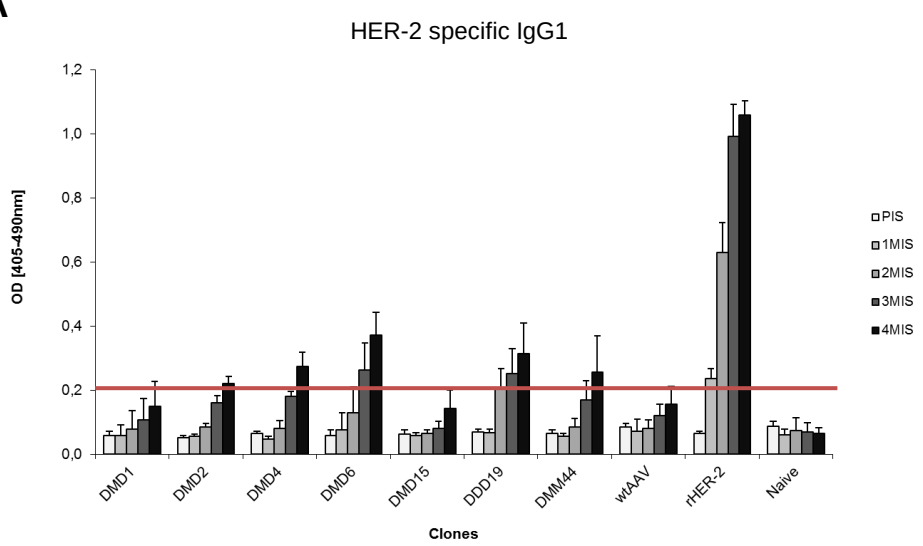

B

4th MIS	vs	Naïve	significance
DMD1		0.009	**
DMD2		0.000	***
DMD4		0.000	***
DMD6		0.000	***
DMD15		0.002	**
DDD19		0.000	***
DMM44		0.000	***
rHER-2		0.000	***

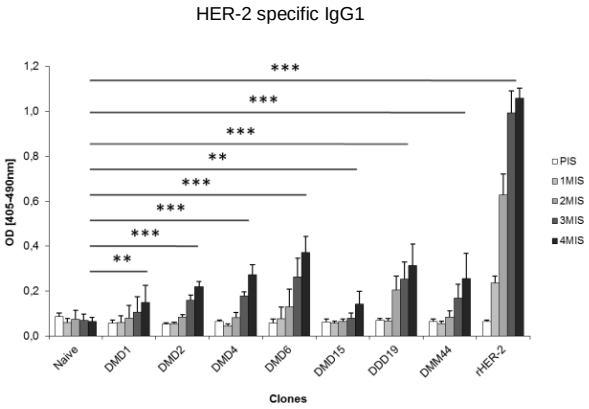

C

4th MIS	vs	wtAAV	significance
DMD1		0.878	ns
DMD2		0.008	**
DMD4		0.000	***
DMD6		0.000	***
DMD15		0.674	ns
DDD19		0.001	**
DMM44		0.036	*
rHER-2		0.000	***

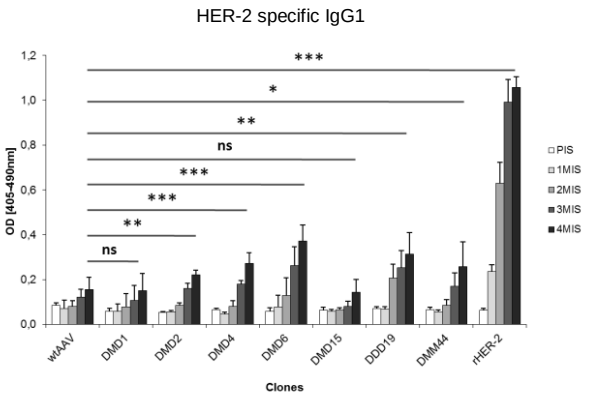

D

PIS	vs	4th MIS	significance
DMD1		0,005	**
DMD2		0.000	***
DMD4		0.000	***
DMD6		0.000	***
DMD15		0.002	**
DDD19		0.000	***
DMM44		0.000	***

wtAAV	0.003	**
rHER-2	0.000	***
Naïve	0.023	*

Figure 3.14: A. Means and standard deviation of IgG1 values determined in single immune sera tested on rHER-2 in ELISA.
Significances comparing B. sera of 4th MIS versus naïve sera, C. 4th MIS versus the group immunized with the carrier particles alone, and D. pre-immune sera versus fourth immune sera.
ns p>0.05; * p<0.05; ** p<0.01; *** p<0.001

3.2.4.2 *Results of transplantation experiment in HER-2 mimotope immunized mice*

A second tumor transplantation experiment was performed after completing four immunizations. This time using only the HER-2 expressing cells D2F2-E2 (1x10^7) which had been controlled for stable HER-2 expression by flow cytometric analysis (not shown). Additionally to the mimotope and HER-2 immunizations one group was treated passively with 4D5 antibody (100µg/mouse). Again, tumors were monitored daily by palpation and caliper measurement during a period of 17 days. However, similar to the first tumor experiment no significances were achieved comparing the single growth curves of differently immunized mice as compared to naïve or wtAAV groups (figure 3.15). The slowest growth curves, however, was achieved by 4D5 antibody. The experiment was interrupted when tumors reached a size of 600mm^3.

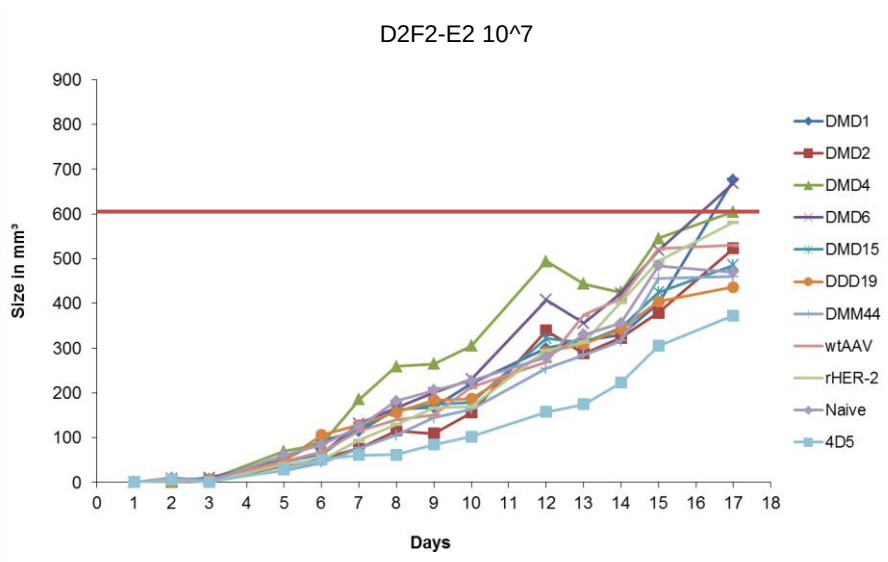

Figure 3.15: Tumor growth curve of D2F2-E2 cells.

3.2.4.3 ***Histology***

In order to find a possible explanation for the failure of the mimotope vaccine experiment grafted tumors were examined histologically for HER-2 expression. Figure 3.16 illustrates a typical appearance of a grafted D2F2-E2 tumor at the inner face of the abdominal skin. Tumors of euthanized naïve (figure 3.17), rHER-2 (figure 3.18) and 4D5 (3.19) mouse groups were removed, paraffinated, cut and histologically stained with Hematoxylin Eosin and with the HercepTest®. Figures 3.18 to 3.20 show typical histochemical results. Each one example representative of the groups of naïve, rHER-2 and 4D5 treated mice is shown. Inside each tumor sections four zones are highlighted: picture A demonstrates marginal area of the skin with sebum glands and hair follicles, were infiltrating lymphocytes were found. Necrosis and ulceration is seen in areas highly stained with eosin, containing blood and damaged tissue (B,C). Picture D contains a high density of tumor cells with prominent nuclei, being colored strongly with hematoxilyn.

Taken together, comparing the HER-2 staining in the different groups did not reveal any difference of expression levels. Thus, failure of target expression did not explain failure of the mimotope vaccination or 4D5 treatment.

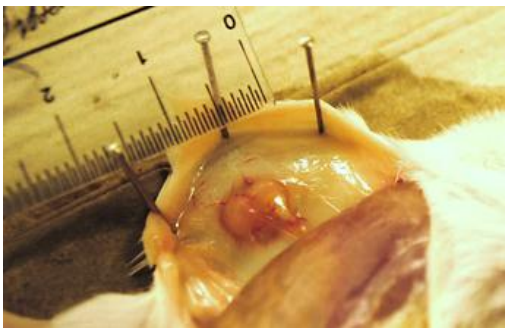

Figure 3.16: Tumor in vivo.

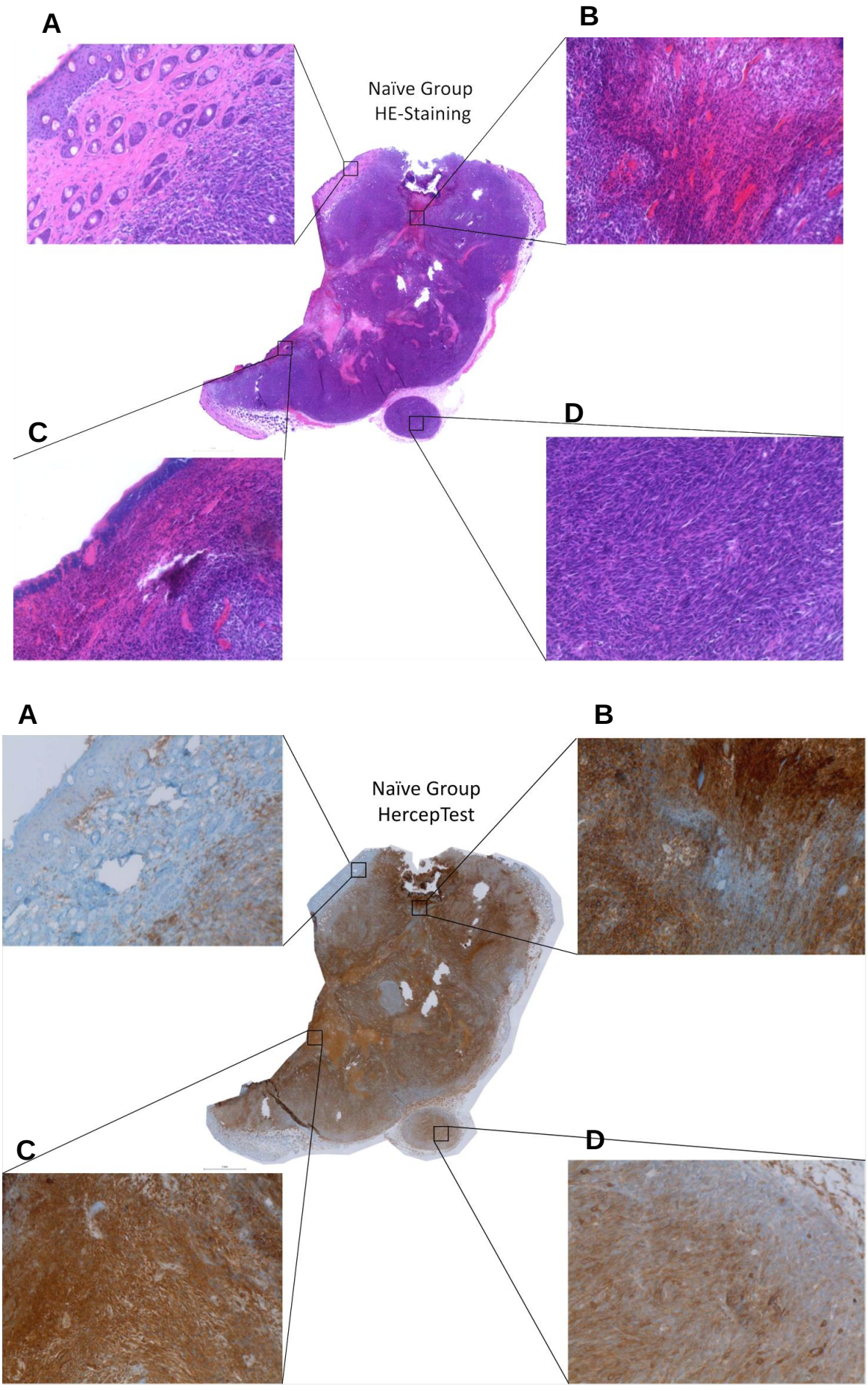

Figure 3.17: Tumor of one representative mouse from naïve group.

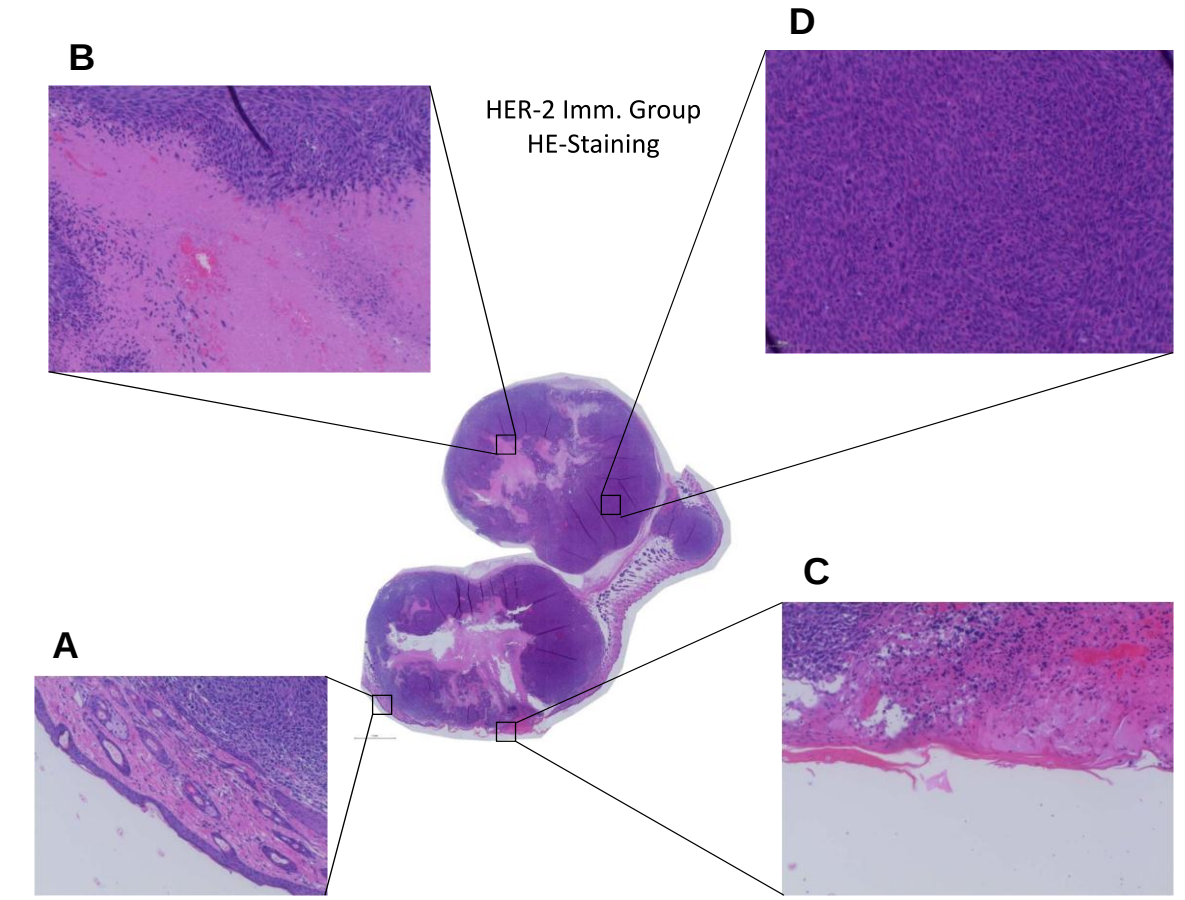

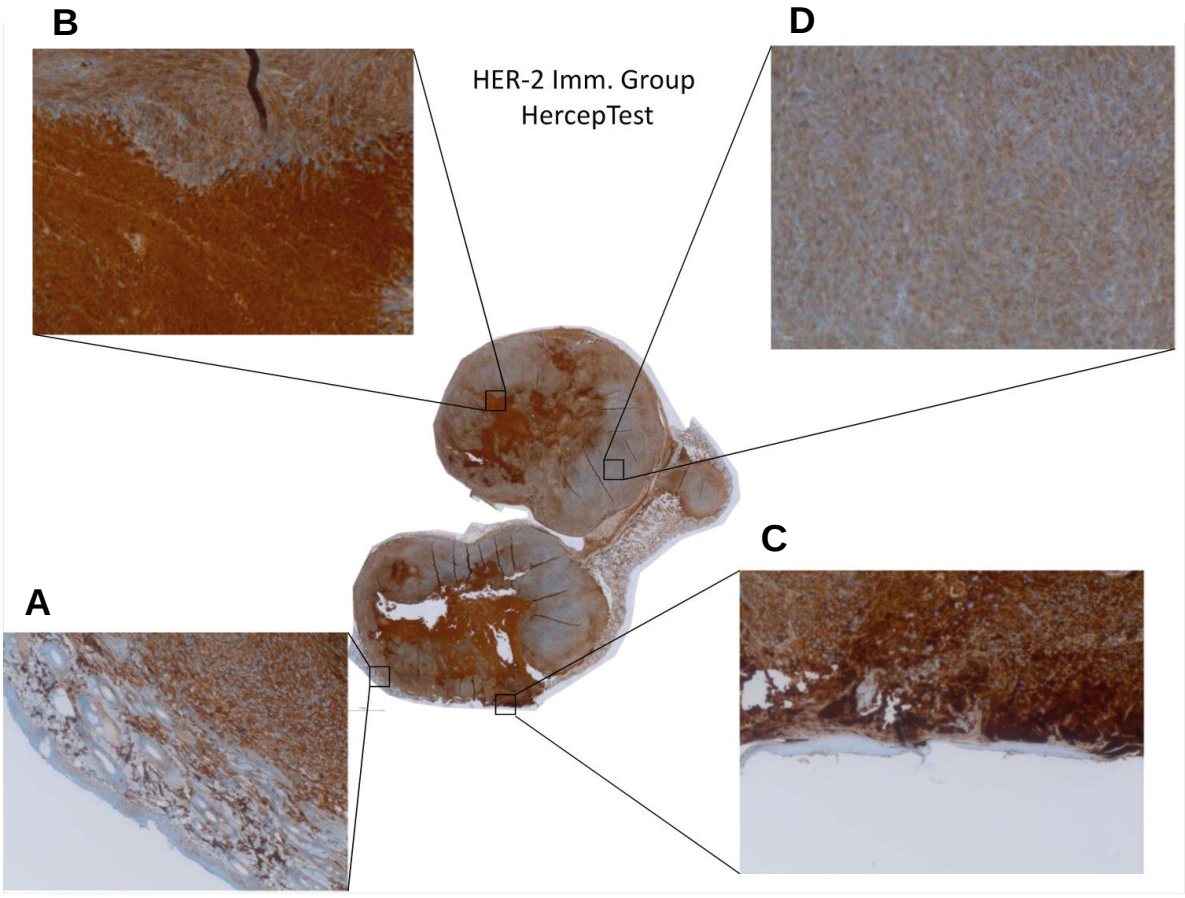

Figure 3.18: Tumor of one representative mouse from with rHER-2 immunized group.

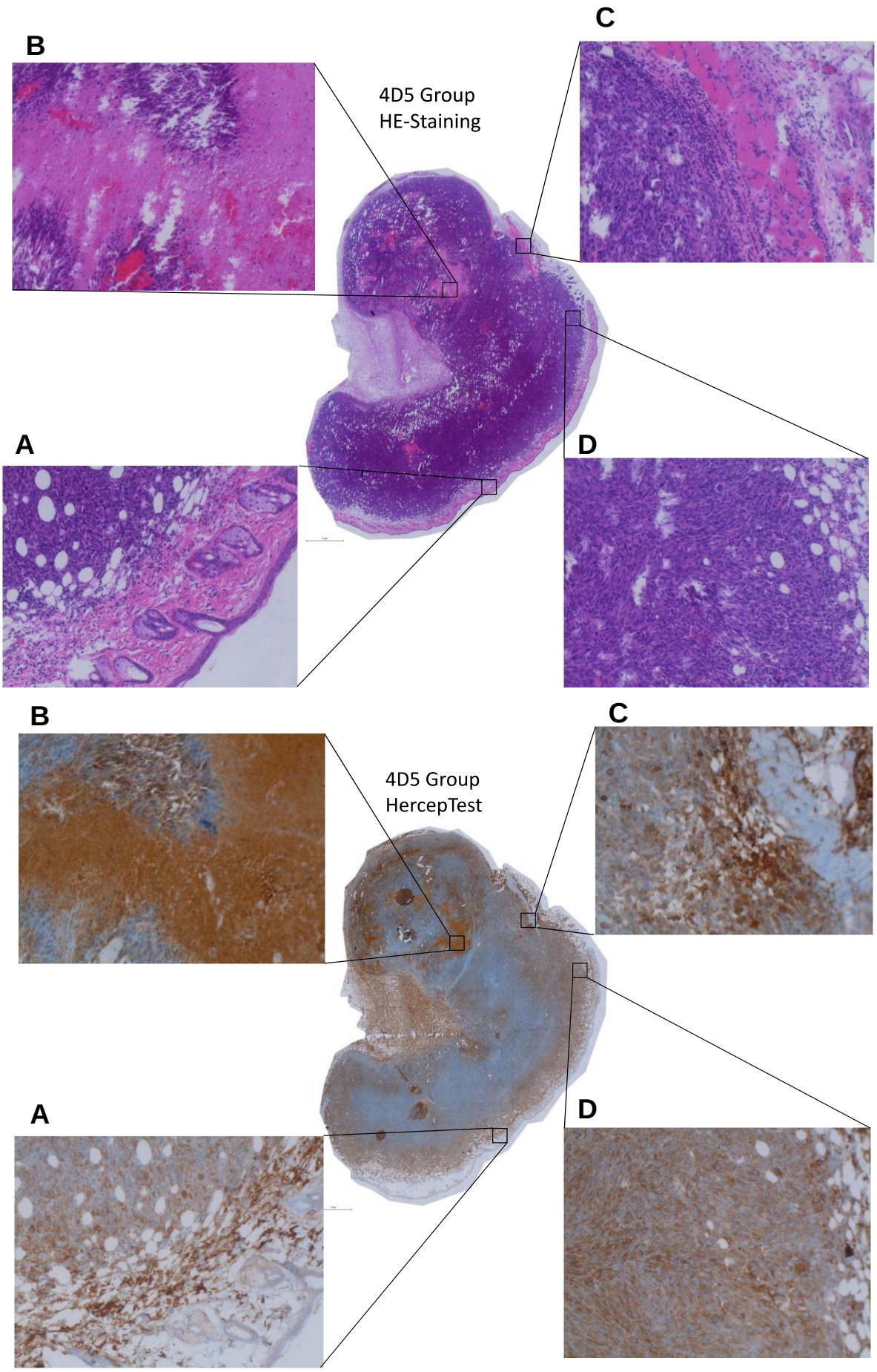

Figure 3.19: Tumor of one representative mouse from group immunized passively with 4D5.

3.2.5 **Proliferation inhibition assay**

From the above it was clear that although the AAV-mimotopes had induced considerable levels of anti-HER-2 antibodies, no biological anti-tumor effect was achieved using HER-2 high expressing cell line D2F2-E2 in the tumor transplant experiment. We therefore considered that D2F2-E2 could be driven by a strong HER-2 independent autonomous oncogenic signal. To verify this, proliferation inhibition experiments were performed using trastuzumab as positive control and for isotype control purposes rituximab and cetuximab. Indeed, neither D2F2-E2 (Fig.3.20 A) nor TAUF1.1 (C) cells, both expressing the HER-2 transgene product on their surface, responded to trastuzumab stimulation. However, when we repeated the experiments with the human natural HER-2 overexpressing cell lines BT474 (E) and mBT474 (F), a significant growth inhibition upon trastuzumab stimulation could be observed after 24h.

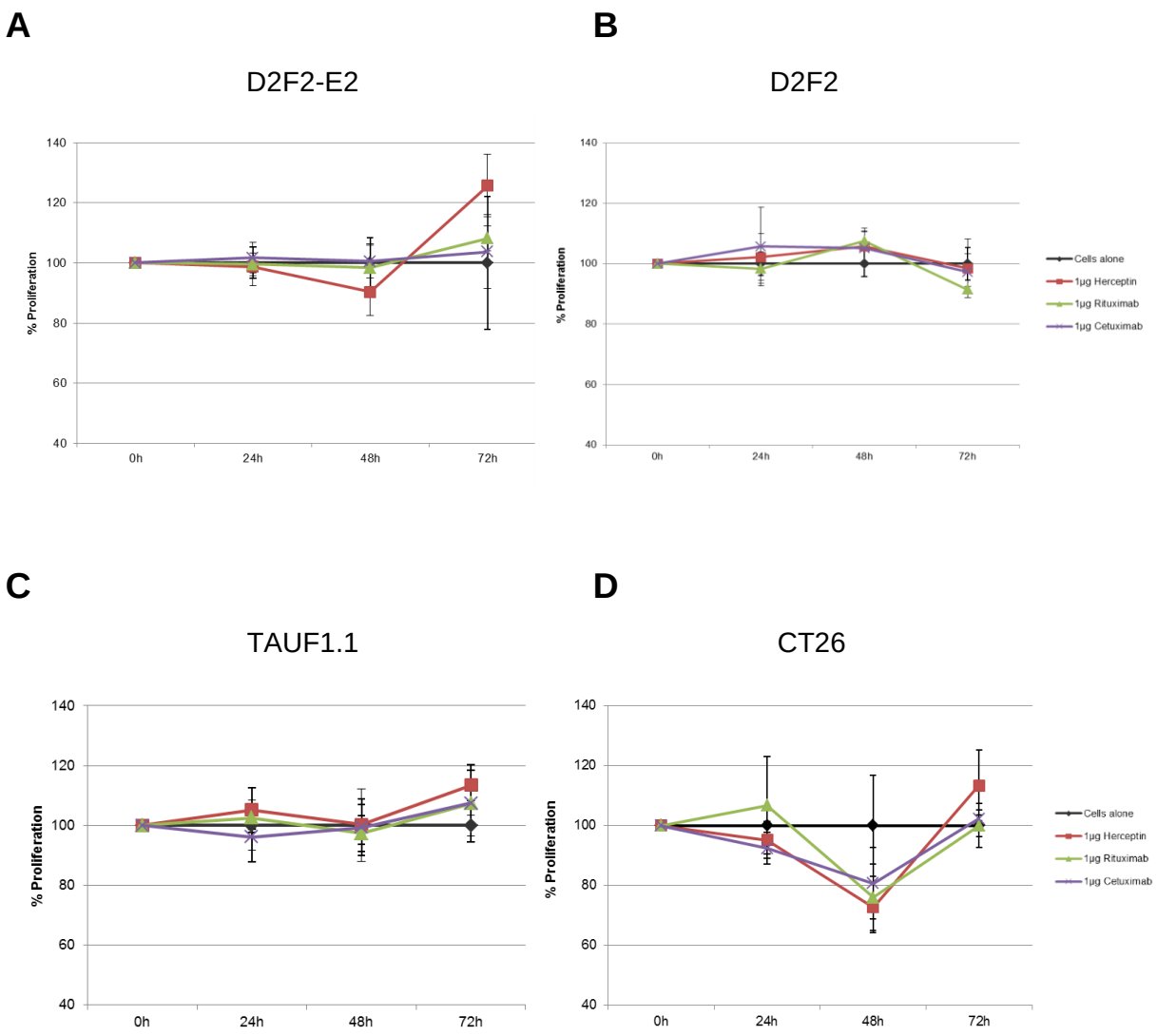

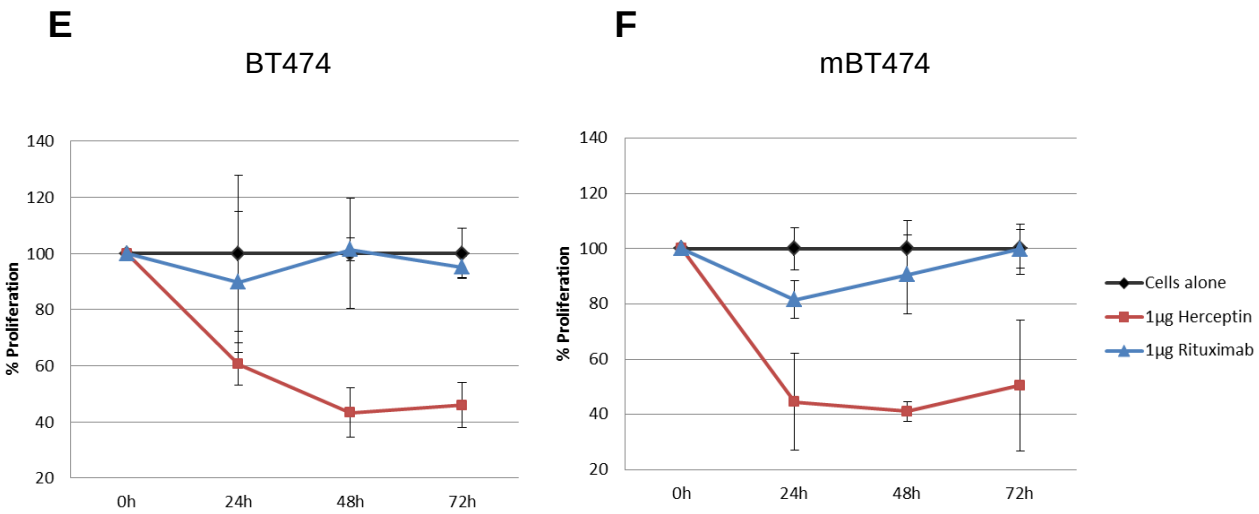

Figure 3.20: Results of proliferation assay of A. D2F2-E2, B. D2F2, C. TAUF1.1, D. CT26, E. BT474 and F. mBT474 cells. BT474 and mBT474 demonstrate a significant proliferation inhibition even after 24h incubation.

3.2.6 **Antibody purification**

The tumor transplant experiment had thus failed due to a non-responsiveness of D2F2-E2 cells to trastuzumab stimulation.

As we considered that the well-responding cells BT474 and mBT474 could not be used for mouse grafting due to their human origin, we decided to prove the functionality of AAV-mimotope induced antibodies by *in vitro* assays. Therefore, we first had to purify IgG from the immune sera showing the highest titers.

Antibodies from pooled preimmune sera and of sera after the forth immunization were purified with protein G sepharose beads; quantified by Pierce BCA protein assay and qualitatively analyzed in non-reducing SDS polyacrylamide gel electrophoresis (data not shown).

Consequently, the specificity of the isolated mouse IgG was controlled by ELISA coated with purified rHER-2 and compared to 4D5 antibody (1µg/ml). Based on the calculated protein amounts in purified IgG fractions, samples were adjusted to 3µg/ml by dilution before incubation. Further, figure 3.21 illustrates that especially the isolated IgG from groups DMD1, DMD2, DMD4 and DMD6 contained IgG1 against HER-2 antigen and were thus suitable for further *in vitro* analyses. Besides IgG1, IgG2a and IgG2b were tested showing only background levels (not shown).

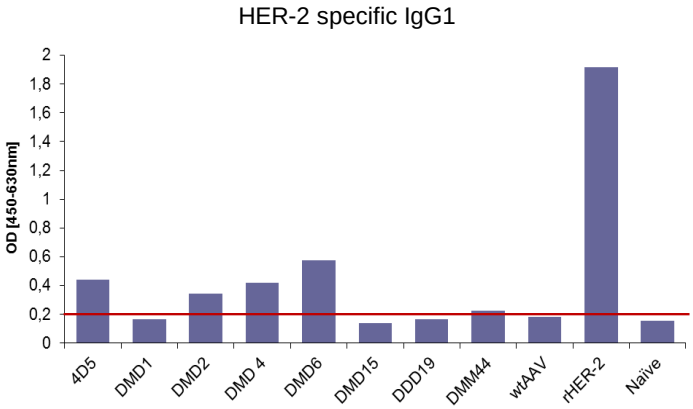

Figure 3.21: IgG1 immune response of purified antibodies 3µg/mL compared to 1µg/mL 4D5 (ELISA). X-axis indicates the mouse groups immunized with different AAV particles, from which IgG was purified. Y-axis shows OD values measured.

Consequently, purified IgG1 from mouse groups immunized with AAV-mimotopes DMD1, DMD2, DMD4, DMD6 were applied in *in vitro* proliferation inhibition assay using BT474 and mBT474 cells. Figure 3.22 illustrates that after 24h incubation antibodies isolated from sera of DMD1 immunized mice induced highly significant growth inhibition in mBT474 and BT474 cells. The effect remained sustained up the 72h in mBT474 cells, but rebound in BT474 cells. In contrast, antibodies from groups DMD4 and DMD6 showed a delayed effect in BT474 cells, but none in mBT474.
In the moment we have no explanation for the different susceptibility of BT474 before and after passaging in SCID mice.

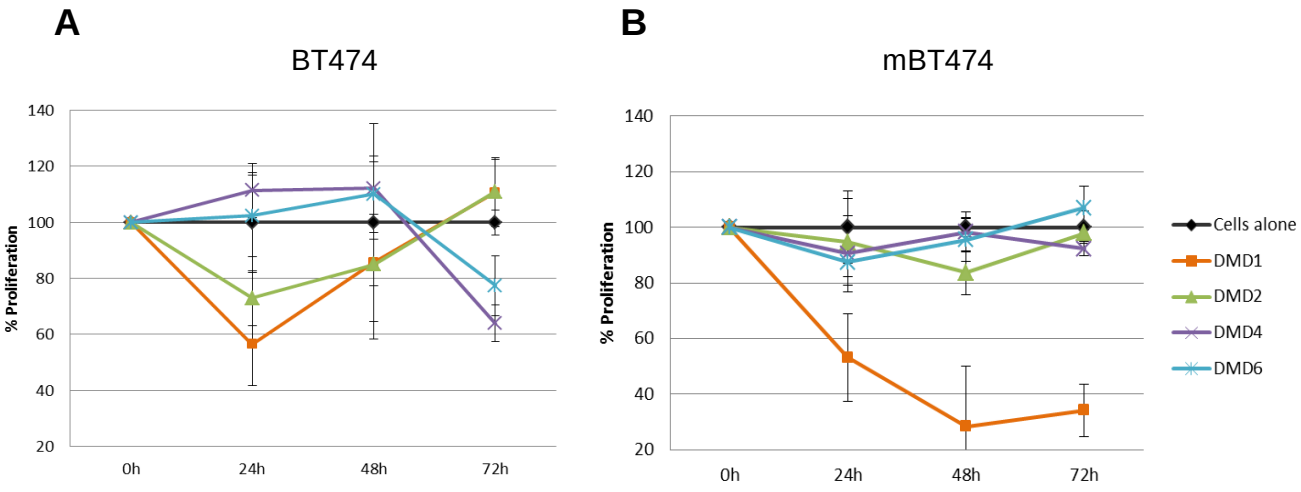

Figure 3.22: Results of proliferations inhibition induced by purified antibodies in A. BT474 and B. mBT474 cells.

Taken together, the AAV-displayed mimotopes were able to induce highly specific anti-HER-2 IgG1 response. The *in vivo* proof of concept failed due to selection of a non-responsive cell line for grafting. However, purified anti-HER-2 mimotope antibodies induced significant growth inhibition in an *in vitro* assay using BT474 and mBT474 cells as responsive tumor targets.

4 Conclusion

Mammary carcinoma is one of the most malignant and common forms of female cancer. In about 25 – 30% of invasive breast cancers and in 70% of ductal carcinoma in situ, the human epidermal growth factor receptor HER-2 is overexpressed. This is associated with a worse prognosis, a decreased survival rate and disadvantages in responses to chemotherapeutic and hormonal anti-cancer agents [3,21].
The advantage, however, in HER-2 overexpressing breast cancer is that targeting of this specific tumor antigen by passive immunotherapy with the humanized monoclonal antibody Herceptin® (trastuzmab) is possible. Trastuzumab binds the extracellular part of HER-2 and thus interferes with the HER-2 activated growth stimulatory signaling pathways. Yet passively applied IgG antibodies are of limited half-life and also their distribution in tissue differs enormously. To circumvent these problems we intended to design an active immunotherapy with memory effects against the HER-2 tumor antigen. Cancer vaccines could be especially attractive for providing protection against recurrence during minimal residual disease. Further, we considered it important that an active immunotherapy should be able to induce antibodies of similar beneficial effects as the original trastuzumab antibody. This aim was pursued by the mimotope concept [22].

Mimotopes are small peptides with similar physical and biochemical properties as the antibody epitope on the original antigen. Tumor mimotopes, including HER-2 mimotopes could already be generated repeatedly by our group utilizing phage-display technology. Because of their low immunogenic activity, they were coupled to carrier molecules like KLH (keyhole limpet hemocyanin) or synthetically produced as octameric MAM (multiple antigenic mimotope). However, both strategies showed some draw backs, such as changes of antigenicity during chemical coupling. Our intention thus here was to optimize mimotopes by using a fusion molecule approach allowing assembling of AAVs and the production of AAVLPs, respectively [35,36].

AAV are replication defective ssDNA viruses, non-pathogenic to humans and consisting of 60 capsomers, which makes them an attractive tool for vaccine technology. For specific surface display VP3 capsid proteins can be assembled to AAVLP with a B-cell epitope of interest. We used a B-cell epitope of ovalbumin as model epitope and compared it to a non-OVA related peptide (TP18) in the first part of the study [40-42].
BALB/c mice were immunized subcutaneously with ovalbumin as positive and AAVLP as negative control groups, further with AAVLP displaying the OVA-B-cell epitope or

AAVLP-TP18 (negative control), and we used either aluminum hydroxide or Montanide ISA 51 as adjuvants.

Our data show that AAVLPs as antigen carriers harbor good immunogenicity, as an anti-carrier response was noticed in AAVLP immunized groups. However, an OVA-specific IgG1 immune response was achieved in AAVLP-OVA immunized groups only. Antibody class IgG2b was only detectable at background levels. This indicated specificity and immunogenicity of the AAVLP OVA model-vaccine.

Next this AAVLP vaccine was tested for safety in respect to IgE induction and triggering of allergy. No IgE towards OVA was induced in AAVLP-OVA immunized group, compared to the positive control (OVA immunized mice). To verify this *in vitro* result a β-hexosaminidase release assay was performed. Thereby, in the presence of IgE RBL cells degranulate upon allergen trigger and release β-hexosaminidase, which can be measured by ELISA. Incubating RBL cells with sera from AAVLP immunized groups, no degranulation was obtained, confirming that no IgE was induced by the AAVLP-OVA vaccine or any of the AAVLP vaccines.

Consequently an *in vivo* anaphylaxis experiment was performed by challenging all mice of each group intravenously with OVA. Rectal temperature typically drops during anaphylaxis and was therefore measured before and after the challenge. A temperature drop was only observed in the OVA-immunized positive control group, whereas all AAVLP immunized mice had a constant body temperature curve during monitoring.

To complete all possible effects of allergy safety, i.e. vaccination safety in an already allergic subject, mice were sensitized i.p. with ovalbumin before they were vaccinated intradermally with different substances. OVA, but also AAVLP-OVA, though less intensely, showed type I skin reaction in the Evan's blue test, while AAVLP alone did not induce Type I skin reactivity. These results indicated that AAVLPs used as carriers for B-cell epitopes have no de novo sensitization capacity. Further, in allergic patients with an allergen-AAVLP vaccine local minor, but no systemic side effects may occur.

The overall aim of this master thesis, however, was to generate a HER-2 specific AAVLP mimotope vaccine. For these proof of concept studies instead of AAVLPs we were forced to used AAVs as display system as many clones had to be screened and

this of course caused manufacturing limitations. First off all immunogenicity and specificity of HER-2 AAV vaccines were evaluated in BALB/c mice. Low but increasing titers of total IgG antibodies against purified rHER-2 were indeed observed in the sera from mice immunized with several of the mimotope clones specific for trastuzumab. When subsequently D2F2-E2 cells were transplanted into them a boost of HER-2 specific IgG due to natural tumor antigen exposure was observed in ELISA as well as in immunofluorescence. This indicated that the HER-2 mimotopes, although of low immunogenicity were able to prime a highly specific IgG anti-HER-2 response.

HER-2 expression of cells had been verified before in flow cytometric analysis and the optimal number of cells to be transplanted by *in vivo* graft titration experiment. D2F2-E2 (a HER-2 expressing murine breast cancer cell line) and D2F2 (its parental form) were subcutaneously transplanted, but D2F2 cells grew aggressively and also started to ulcerate from day 10, which forced us to terminate the experiment.

Therefore, a second immunogenicity and specificity study was planned thoroughly, adding new and possibly better HER-2 mimotope clones, using this time four instead of three immunization rounds and Alum as an alternative adjuvant. ELISA results demonstrated a significant increase in IgG1 antibodies against rHER-2 compared to wtAAV or naïve groups.

Consequently, the tumor transplant experiment was repeated, using only D2F2-E2 for transplantation without the heavily growing parental cell line D2F2. Although the experimental procedure had been improved, again no significances between tumor growth of different groups, could be achieved. Our immunohistological analysis using HercepTest® of tumors indicated that the treatment failure could not be explained by HER-2 down regulation during the experiment. It seemed thus probable that D2F2-E2 cells, expressing HER-2 as a transgene product were not responding to HER-2 targeting. To check that, murine HER-2 expressing D2F2-E2 and TAUF1.1 cells, in comparison to naturally overexpressing tumor cells BT474 and mBT474 were *in vitro* stimulated with trastuzumab and proliferation reacted as compared to isotype controls. Indeed, only human cancer cells showed significant and sustained proliferation inhibition.

Hence, HER-2 was neither expressed functionally on D2F2-E2 nor on TAUF1.1 cells, providing an explanation for the failure of the *in vivo* experiment. This result suggests

that our HER-2 mimotope vaccine might be effective in the right model. Therefore, BT474 and mBT474 cell lines (the later being once transferred through a SCID mouse) were used for a proliferation inhibition assay using this time IgG antibodies purified from mimotope-immunized mice. Purified antibodies of clone DMD1 resulted in mBT474 tumor growth inhibition, equivalent to effects achieved with trastuzumab. Further, on BT474 cells the purified IgG induced by immunizing with AAV mimotope clones DMD4 and DMD6 showed anti-proliferative effects. These results thus evidenced *in vitro* tumor inhibitory effects of the AAV HER-2 mimotope vaccines when using responsive cell lines. As we considered that human BT474 cells cannot be transplanted into mice, an appropriate *in vivo* proof of concept is to this date still missing.

Taken all data together, HER-2 mimotope AAVs are, in concert with the right adjuvant, highly immunogenic and able to actively induce immune responses to the specific antigenic epitope. AAV-display further does not prompt de novo sensitization. This master thesis thus presents a novel and safe approach using AAV-displayed HER-2 mimotope for channeling the immune system towards a specific and strong response.

References

1 Alberts B. et al. Molecular biology of the cell. 5th edition, Garland Science New York and London (2008)

2 GLOBOCAN World cancer report http://globocan.iarc.fr/factsheets/populations/factsheet.asp?uno=900

3 World health Organization. Breast cancer: prevention and control. http://www.who.int/cancer/detection/breastcancer/en/index1.html

4 Pollán M. et al. Epidemiology of breast cancer in young women. *Breast Cancer Res Treat* **123**: 3-6 (2010)

5 Von Euler-Chelpin M. et al. Breast cancer incidence and use of hormone therapy in Denmark 1978-2007. *Cancer Causes Control* **22**: 181-7 (2011)

6 Giordano SH. et al. Breast carcinoma in men: a population based study. *Cancer* **101**(1): 51-7 (2004)

7 Faller A. et al. Der Körper des Menschen 14th edition Thieme (2004)

8 Patrick J. Lynch, medical illustrator, female breast http://patricklynch.net/portfolios/medical-illustration/content/breast_anatomy_normal_Copyright_Lynch_2007_large.html

9 Kelley W. Textbook of Internal Medicine, Lippincott-Raven Publishers, Philadelphia, New York, (1997).

10 Singletary E. et al. Revision of the American Joint Committee on Cancer Staging System for Breast Cancer. *J Clin Oncol* **20**: 3628-3636 (2002).

11 Farhat GN. Sex hormone levels and risks of estrogen receptor-negative and estrogen receptor-positive breast cancers. *J Natl Cancer Inst* **103**(7): 562-70 (2011)

12 Madigan MP. et al. Proportion of breast cancer cases in the United States explained by well-established risk factors. *J Natl Cancer Inst* **87**(22): 1681-5 (1995)

13 Chlebowski RT. Lifestyle and breast cancer risk: the way forward? *J Clin Oncol* **28**(9): 1445-7 (2010)

14 Phipps AL. et al. Reproductive history and oral contraceptive use in relation to risk of triple-negative breast cancer. *J Natl Cancer Inst* **103**(6): 470-7 (2011)

15 Hall JM. et al. Linkage of early-onset familial breast cancer to chromosome 17q21. *Sience* **250**(4988): 1684-9 (1990)

16 Wooster R. et al. Localization of a breast cancer susceptibility gene, BRCA2, to chromosome 13q12-13. *Sience* **265**(5181): 2088-90 (1994)

17 Duncan JA. et al. BRCA1 and BRCA2 proteins: roles in health and disease. *Mol Path* **51**: 237-47 (1998)

18 Baxter N. et al. Preventive health care, 2001 update: should women be routinely taught breast self-examination to screen for breast cancer? *CMAJ* **164**(13): 1837-46 (2001)

19 Schmidinger, M. Mammakarzinom. (Vienna).

20 Sotiriou C. Gene-Expression Signatures in Breast Cancer. *N Engl J Med* **360**: 790-800 (2009)

21 Slamon DJ. et al., Studies of the HER-2/neu proto-oncogene in human breast and ovarian cancer. *Science* **244**: 707-12 (1989)

22 Hudis CA. et al. Trastuzumab – Mechanisms of action and use in clinical practice. *N Engl J Med* **357**: 39-51 (2007)

23 Yarden Y. et al. Biology of HER2 and its importance in breast cancer. *Oncology* **61**(2): 1-13 (2001)

24 Yarden Y. et al. The EGFR family and its ligans in human cancer: signaling mechanisms and therapeutic opportunities. *Eur J Cancer* **37**(4): 3-8 (2001)

25 Greenberg CC et al. Institutional Variation in the Surgical Treatment of Breast Cancer: A Study of the NCCN. *Ann Surg* (2011)

26 Belletti B. et al. Targeted intraoperative radiotherapy impairs the stimulation of breast cancer cell proliferation and invasion caused by surgical wounding. *Clin Cancer Res* **14**(5): 1325-32 (2008)

27 Jordan VC. et al. Tamoxifen (ICI46,474) as a targeted therapy to treat and prevent breast cancer. *Br J Pharmacol* **147**(1): 269-76 (2006)

28 Atkins CD. et al. Optimal chemotherapy for high-risk early-stage breast cancer. *J Clin Oncol* **28**(16): e263 (2010)

29 Janeway C. et al. Immunobiology. 7th edition, Garland Science Publishing, New York and London (2008)

30 Valabrega G. et al. Trastuzumab: mechanism of action, resistance and future perspectives in HER2-overexpressing breast cancer. *Ann Oncol* **18**(6): 977-84 (2007)

31 Cho HS. et al. Structure of the extracellular region of HER2 alone and in complex with the Herceptin Fab. *Nature* **421**, 756-760 (2003)

32 Carter, P., et al. Humanization of an anti-p185HER2 antibody for human cancer therapy. *Proc Natl Acad Sci U S A* **89**: 4285-9 (1992)

33 Riemer AB. et al. Matching trastuzumab (Herceptin®) epitope mimics onto the surface of Her-2/neu - a new method of epitope definition. *Mol Immunol* **42**(9): 1121-4 (2005)

34 Riemer AB. et al. Generation of Peptide mimics of the epitope recognized by trastuzumab on the oncogenic protein Her-2/neu. *J Immunol* **173**(1): 394-401 (2004)

35 Knittelfelder R. et al. Mimotope vaccination – from allergy to cancer. *Expert Opin Biol Ther* **9**(4): 493-506 (2009)

36 Riemer AB. et al. Mimotope vaccines: Epitope mimics induce anti-cancer antibodies. *Immunol Lett* **113**: 1-5 (2007)

37 Yip YL. et al. Identification of epitope regions recognized by tumor inhibitory and stimulatory anti-ErbB-2 monoclonal antibodies: implications for vaccine design. *J Immunol* **166**(8): 5271-8 (2001)

38 Brämswig KH. et al. Immunization with mimotopes prevents growth of carcinoembryonic antigen positive tumors in BALB/c mice. *Clin Cancer Res* **13**(21): 6501-8 (2007)

39 DMHC2531 Stakeholder Opinions, Vaccine Antigen Delivery (05/2009) www.datamonitor.com/store/Download/Brochure/?productId=DMHC2531

40 Chackerian B. et al. Virus – like particles: flexible platforms for vaccine development. *Expert Rev Vaccines* **6**(3): 381-90 (2007)

41 Xie Q. et al. The atomic structure of adeno-associated virus (AAV-2), a vector for human gene therapy. *Proc Natl Acad Sci U S A* **99**(16): 10405-10 (2002)

42 Madsen D. et al. Adeno-associated virus serotype 2 induces cell-mediated immune responses directed against multiple epitopes of the capsid protein VP1. *J Gen Virol* **90**(Pt 11): 2622-33 (2009)

43 Baltimore D. et al. Expression of animal virus genomes. Bacteriol Rev 35(3): 235-41 (1971)

44 Schultz BR. et al. Recombinant adeno-associated virus transduction and integration. *Mol Ther* **16**(7): 1189-99 (2008)

45 Qiu J. et al. The interaction of heparin sulfate and adeno-associated virus 2. *Virology* **269**(1): 137-47 (2000)

46 Pajusola K. et al. Cell-type-specific characteristics modulate the transduction efficiency of adeno-associated virus type 2 and restrain infection of endothelial cells. *J Virol* **76**(22): 11530-40 (2002)

47 Michels KB. et al. HPV vaccine for all. Lancet 374(9686):268-70 (2009)

48 Padron E. et al. Structure of adeno-associated virus type 4. *J Virol* **79**(8): 5047-58 (2005)

49 Grgacic EV et al. Virus-like particles: passport to immune recognition. *Methods* **40**(1): 60-5 (2006)

50 Key facts of AAVLPs. http://www.medigene.de/aavlp/

51 Brunner R. et al. The ABC of clinical and experimental adjuvants – A brief overview. *Immunol Lett* **128**(1): 29-35 (2010)

52 Jang SI. et al. Montanide™ ISA 71 VG adjuvant enhances antibody and cell-mediated immune responses to profilin subunit antigen vaccination and promotes protection against Eimeria acervulina and Eimeria tenella. *Exp Parasitol* **127**(1): 178-83 (2011)

53 Hanly WC. et al. Overview of Adjuvants: Advantages and disadvantages. http://www.nal.usda.gov/awic/pubs/antibody/overview.htm

54 Renz H. et al. Comparison of the allergenicity of ovalbumin and ovalbumin peptide 323-339. Differential expansion of V beta-expressing T cell populations. *J Immunol* **151**(12): 7206-7213 (1993)

Table of Figures

List of Tables

Abbreviations

aa	Amino acid
AAV	Adeno-associated virus
AAVLP	Adeno-associated virus-like particle
ADCC	Antibody dependent cell mediated cytotoxicity
AG	Antigen
AJCC	American Joint Committee on Cancer Staging
Alum	Aluminum hydroxide
APC	Antigen presenting cell
AR	Amphiregulin
BRCA1,2	Breast cancer antigen 1, 2
CDC	Complement dependent cytotoxicity
CEA	Carcino embryonic antigen
CTL	Cytotoxic T-cell
(k)Da	(kilo) Dalton
DCIS	Ductal carcinoma in situ
DNA	Desoxyribonuleinacid
EGF	Epidermal growth factor
EGFR	Epidermal growth factor receptor
ELISA	Enzyme-linked immunosorbent assay
EPR	Epiregulin
ER	Estrogen receptor
FCS	Fetal calf serum
FDA	Food and Drug Administration
FGF	Fibroblast growth factor
G418	Geneticin
HB-EGF	Heparin binding epidermal growth factor
HE	Hematoxilyn Eosin
HER-2	Human epidermal growth factor receptor 2
HRP	Horse radish peroxidase
IgG/E	Immunoglobulin class G/E
IL	Interleukin
ISCOM	Immune stimulating complexes
KLH	Keyhole limpet hemocyanin
LCIS	Lobular carcinoma in situ
MAM	Multiple antigenic mimotope

MAP	Multiple antigenic peptide system
MAPK	Mitogen activated protein kinase
MHC I/II	Major histocompatibility complex class I/II
Mont	Montanide ISA 51 VG®
NRG	Neuregulin
OVA	Ovalbumin
p95	Protein 95kDa
PBS	Phosphat buffered saline
PDGF	Platelet derived growth factor
PI3-Kinase	Phosphoinositol 3-Kinase
PR	Progesteron receptor
RTK	Receptor tyrosine kinase
SDS-PAGE	Sodiumdodecylsulfat Polyacrylamid gelelectrophoresis
TBST	Tris buffered saline 0.05% Tween
TGF-α	Transforming growth factor α
T_H-1/2	T-helper cell ½
Tis	Tumor in situ
TP18	Cholesterolester transferprotein 18
TTSN	Random peptide sequence
UICC	Union for International Cancer Control
VEGF	Vascular endothelial growth factor
VLP	Virus-like particles
VP3	Viral protein 3 (capsid protein)

Curriculum Vitae

Persönliche Angaben

Name:	Kathrin Thell
Geburtsdatum:	07. Oktober 1985
Geburtsort:	Wien
Staatsbürgerschaft:	Österreich
Wohnort:	7152 Pamhagen
E-Mail:	kathrin.thell@meduniwien.ac.at
Eltern:	Michael (1961) und Katharina (1965) Thell
Geschwister:	Schwester, Birgit Thell (1989)

Schulische Ausbildung

seit Okt. 2007	Molekulare Biologie an der Universität Wien Schwerpunkt: Molekulare Medizin
2004 – 2007	Akademie für den medizinisch-technischen Laboratoriumsdienst am Allgemeinen Krankenhaus der Stadt Wien Diplom für biomedizinische Analytik mit ausgezeichnetem Erfolg
2000 – 2004	Bundesgymnasium (Oberstufe) in Neusiedl/See
1996 – 2000	Bundesgymnasium (Unterstufe) in Neusiedl/See
1992 – 1996	Volksschule in Pamhagen

Besondere Kenntnisse

Sprachen:	Deutsch (Muttersprache) Englisch Latein Italienisch Französisch (Grundkenntnisse)
EDV:	gute MS Office Kenntnisse gute Apple Macintosh Kenntnisse SPSS und GraphPad Prism: Dateneingabe und einfache statistische Berechnungen

Mitgliedschaft

Österreichische Gesellschaft für Allergologie und Immunologie (ÖGAI)

Berufserfahrung

Juli 2007 – Dez. 2008	Karl Landsteiner Institut für Zellbiologie und Zelltherapie in der Krankenanstalt Rudolfstiftung in Wien Kultivierung und Charakterisierung von hämatopoetischen Stammzellen Betreuung einer Diplomandin der MTA Akademie
seit Sept. 2010	Biomedical International R+D, Institut für Pathophysiologie und Allergieforschung, Medizinische Universität Wien Proof of concept studies for tumor mimotope vaccines

Kongressteilnahme

Zentrumsymposium des Zentrums für Pathophysiologie, Infektiologie und Immunologie (CePII), September 2010 in Wien

Jahrestagung der österreichischen Gesellschaft für Allergologie und Immunologie (ÖGAI), Dezember 2010 in Wien

Communication in Health and Disease (CCHD) Symposium “Bridging the Gap”, Februar 2011 in Wien

7th Young Science Association (YSA) PhD Symposium, Juni 2011 in Wien
Poster Präsentation, Abstract:

Thell K., Szalai K., Singer J., Ritter M., Pfanzagl B., Willensdorfer A., Stremnitzer C., Michaelis U., Jensen-Jarolim E.
Adeno-associated virus-like particles (AAVLPs) as carriers for B-cell vaccines: Immunogenicity and safety aspects

Jahrestagung der österreichischen Gesellschaft für Allergologie und Immunologie (ÖGAI), September 2011 in Graz
Poster Präsentation, Abstract:

Thell K., Szalai K., Singer J., Ritter M., Pfanzagl B., Willensdorfer A., Stremnitzer C., Michaelis U., Jensen-Jarolim E.
New carriers for B-cell vaccines: Immunogenicity and safety aspects Adeno-associated virus-like particles (AAVLPs)

Singer J.*, Szalai K.*, **Thell K.**, Willensdorfer A., Stremnitzer C., Szöllösi H., Michaelis U., Weghofer M., Jensen-Jarolim E.
Evaluation of anti-tumor vaccines using Adeno-associated virus like particles (AAVLP) as carrier for HER-2 mimotopes

Zentrumsymposium des Zentrums für Pathophysiologie, Infektiologie und Immunologie (CePII), September 2011 in Wien
Poster Präsentation, Abstract:

Thell K., Szalai K., Singer J., Ritter M., Pfanzagl B., Willensdorfer A., Stremnitzer C., Michaelis U., Jensen-Jarolim E.
Immunogenicity and safety aspects Adeno-associated virus-like particles: new carriers for B-cell vaccines

Singer J.*, Szalai K.*, **Thell K.**, Willensdorfer A., Stremnitzer C., Szöllösi H., Michaelis U., Weghofer M., Jensen-Jarolim E.
Evaluation of Adeno-associated virus like particles (AAVLP) as carrier for HER-2 mimotope cancer vaccines

XXII World Allergy Congress, Dezember 2011 in Cancun, Mexiko
Jensen-Jarolim E., Szalai K., **Thell K.**, Singer J., Ritter M., Pfanzagl B., Willensdorfer A., Stremnitzer C., Michaelis U.
Immunogenicity and safety aspects of adeno-associated virus-like particles (AAVLPs) as carriers for B-cell vaccines

10th EAACi-Ga2len Immunology Winter School, Februar 2012 in Åre, Schweden
Singer J., Szalai K., **Thell K.**, Ritter M., Pfanzagl B., Willensdorfer A., Stremnitzer C., Michaelis U., Jensen-Jarolim E.
Evaluation of Immunogenicity and safety aspects of Adeno-associated virus-like particles (AAVLPs) as carriers for B-cell vaccines in an OVA-allergy model